# Title: SARS-CoV-2 correlates of protection from infection against variants of concern

**Author list:** Kaiyuan Sun[1†*], Jinal N. Bhiman[2,3†], Stefano Tempia[4,5,6], Jackie Kleynhans[4,5], Vimbai Sharon Madzorera[2,3], Qiniso Mkhize[2,3], Haajira Kaldine[2,3], Meredith L McMorrow[6,8], Nicole Wolter[4,7], Jocelyn Moyes[4,5], Maimuna Carrim[4,7], Neil A Martinson[9,10], Kathleen Kahn[11], Limakatso Lebina[9], Jacques D. du Toit[11], Thulisa Mkhencele[4], Anne von Gottberg[4,7], Cécile Viboud[1‡], Penny L. Moore[2,3,12‡], Cheryl Cohen[4,5‡*], PHIRST-C group[#]

**Affiliations:**

[1]Division of International Epidemiology and Population Studies, Fogarty International Center, National Institutes of Health, Bethesda, Maryland, United States of America.

[2]SAMRC Antibody Immunity Research Unit, University of the Witwatersrand, Johannesburg, South Africa

[3]Centre for HIV and STIs, National Institute for Communicable Diseases of the National Health Laboratory Service, Johannesburg, South Africa

[4]Centre for Respiratory Diseases and Meningitis, National Institute for Communicable Diseases of the National Health Laboratory Service, Johannesburg, South Africa.

[5]School of Public Health, Faculty of Health Sciences, University of the Witwatersrand, Johannesburg, South Africa.

[6]Influenza Division, Centers for Disease Control and Prevention, Atlanta, Georgia, United States of America.

[7]School of Pathology, Faculty of Health Sciences, University of the Witwatersrand, Johannesburg, South Africa.

[8]COVID-19 Response, Centers for Disease Control and Prevention, Atlanta, Georgia, United States.

[9]Perinatal HIV Research Unit, University of the Witwatersrand, South Africa.

[10]Johns Hopkins University Center for TB Research, Baltimore, Maryland, United States of America.

[11]MRC/Wits Rural Public Health and Health Transitions Research Unit (Agincourt), School of Public Health, Faculty of Health Sciences, University of the Witwatersrand, Johannesburg, South Africa.

[12]Centre for the AIDS Programme of Research in South Africa (CAPRISA), Durban, South Africa

†These authors contributed equally.

‡These authors jointly supervised this work.

*Corresponding authors. Email: kaiyuan.sun@nih.gov (KS); cherylc@nicd.ac.za (CC)

[#]A list of authors and their affiliations appears at the end of the paper.

## Abstract

Serum neutralizing antibodies (nAbs) induced by vaccination have been linked to protection against symptomatic COVID-19 and severe disease. However, much less is known about the efficacy of nAbs in preventing the acquisition of infection, especially in the context of natural immunity and against SARS-CoV-2 immune-escape variants. In this study, we conducted mediation analysis to assess serum nAbs induced by prior SARS-CoV-2 infections as potential correlates of protection (CoPs) against Delta and Omicron BA.1/2 wave infections, in rural and urban household cohorts in South Africa. We find that, in the Delta wave, anti-D614G nAbs mediate 37% (95%CI 34% – 40%) of the total protection against infection conferred by prior exposure to SARS-CoV-2, and that protection decreases with waning immunity. In contrast, anti-Omicron BA.1 nAbs mediate 11% (95%CI 9 – 12%) of the total protection against Omicron BA.1/2 wave infections, due to Omicron's neutralization escape. These findings underscore that CoPs mediated through nAbs are variant-specific, and that boosting of nAbs against circulating variants might restore or confer immune protection lost due to nAb waning and/or immune escape. However, the majority of immune protection against SARS-CoV-2 conferred by natural infection cannot be fully explained by serum nAbs alone. Measuring these and other immune markers including T-cell responses, both in the serum and in other compartments such as the nasal mucosa, may be required to comprehensively understand and predict immune protection against SARS-CoV-2.

## Main text

The acute phase of the COVID-19 pandemic has waned with the development of SARS-CoV-2 population immunity in most individuals through repeated episodes of vaccination, infection, or both [1,2]. Owing to the unprecedented speed of SARS-CoV-2 vaccine development and distribution [3], considerable numbers of people were primed by vaccination, averting substantial morbidity and mortality [4]. However, due to immune evasive variants, vaccine hesitancy, and lack of global equity in vaccine access [5–7], a substantial proportion of the world's population acquired SARS-CoV-2 immunity through natural infections, especially in low- and middle-income countries [8,9]. Immune markers that reliably predict protection from infection or symptomatic disease are known as "correlates of protection" (CoP). The post-pandemic era is marked by rapid antigenic drift of Omicron subvariants leading to continued immune evasion [10–13]. Given this complex evolutionary landscape, it remains important to identify CoPs induced by natural infections and/or vaccinations against SARS-CoV-2 variants to monitor population susceptibility, anticipate future waves, optimize rollout of existing vaccines, and facilitate design and approval of next generation vaccines [14]. There has been significant progress in defining serum neutralizing or binding antibodies to the spike protein as CoPs for COVID-19 vaccines, although most of the data are derived from early randomized controlled trials focused on peak immune response shortly after vaccination and measured against symptomatic disease caused by the ancestral strain, with updated data on variants [15–24]. In comparison, little is known about serum CoPs for infection-induced immunity and protection against acquisition of subclinical infections.

CoPs may differ for immunity induced by infection vs. vaccination: SARS-CoV-2 infections tend to induce more robust mucosal immunity despite lower serum antibody responses than intramuscularly delivered mRNA vaccines, as shown in a mouse model [25], and mucosal immunity may play a more important role in reducing risk of infection and transmission than systemic immunity [26,27]. Moreover, CoPs need to be interpreted in the context of viral evolution: in the pre-Omicron era, SAR-CoV-2 variants of concerns emerged independently from one another, with the Alpha, Beta, Gamma, Delta, and Omicron variants exhibiting distinct phenotypic characteristics. The Omicron variant stands out due to substantial genetic divergence from earlier strains and significant immune evasion capabilities against antibody neutralization [28]. Equivalent antibody titers may not provide equivalent levels of protection against ancestral strains compared to more

84 transmissible and immune-evasive variants like Omicron, and CoPs may therefore be variant-
85 dependent. Furthermore, serum antibody titers against SARS-CoV-2 also wane with time.

86 The challenge of defining CoP for infection induced immunity partially stems from the difficulty
87 of tracking immune exposures to SARS-CoV-2 infections, given that a significant proportion of
88 infections are asymptomatic or subclinical and cannot be fully captured by traditional symptom-
89 based surveillance protocols. The SARS-CoV-2, influenza, and respiratory syncytial virus
90 community burden, transmission dynamics, and viral interaction in South Africa (PHIRST-C)
91 cohorts in South Africa [29,30] overcame this challenge by implementing a rigorous sampling
92 strategy, including collection of nasal swabs twice-weekly during a period of intense follow up,
93 along with a total of 10 sequential blood draws spanning the D614G, Beta, Delta, and Omicron
94 BA.1/2 waves. This high-intensity sampling scheme allowed us to reconstruct the cohort
95 participants' SARS-CoV-2 infection histories with high fidelity, and to monitor infection-induced
96 antibody responses over time [30]. Blood samples collected immediately prior to Delta and Omicron
97 waves offered a unique opportunity to investigate serum immune marker levels in close proximity
98 to the next SARS-CoV-2 exposure. Furthermore, vaccine-derived immunity remained low at the
99 onset of the Omicron BA.1/2 wave, with less than 25% of the population fully immunized with
100 Ad26.COV2.S (Janssen) and/or BNT162b2 (Pfizer BioNTech) vaccines [31]. In this study, we
101 leveraged the PHIRST-C cohorts' unique serological and epidemiological data to perform
102 mediation analysis and assess neutralizing antibody (nAb) titers induced by prior infection as CoPs
103 against variants of concerns. Specifically, we evaluated the role of anti-D614G and anti-Omicron
104 BA.1 nAbs against the Delta and Omicron BA.1/2 variants.

105

106 ## Results

107 ### Cohort description and antibody titer measurements

108 We analyzed data from the multi-year PHIRST-C cohort study, covering the first four waves of
109 SARS-CoV-2 infections including the Delta and Omicron BA.1/2 waves [29,30]. The study included
110 a rural and an urban site in two provinces of South Africa. Households with more than two
111 members and where at least 75% of members consented to participate were eligible. A total of
112 1200 individuals from 222 randomly selected and eligible households among the two study sites
113 were longitudinally followed from June 2020 through April 2022. The study was characterized by

114 intense nasopharyngeal swab and serum sample collection from the peak of the SARS-CoV-2
115 D614G (1st) wave to after the peak of the Delta (3rd) wave. After this initial follow-up period,
116 nasopharyngeal swab sample collection stopped but serum samples continued with blood drawn
117 immediately following the Omicron BA.1/2 (4th) wave. The timing of the serum sample collection
118 is visualized in Fig. 1. We previously reconstructed the detailed SARS-CoV-2 infection history of
119 each individual in the cohort up to the Omicron BA1/2 wave and demonstrated that immunity
120 conferred by prior infection reduced the risk of reinfection [30,32]. In this study, we extended this
121 work to investigate how infection-induced neutralizing antibody (nAb) titers correlate with
122 protection against SARS-CoV-2 reinfection with the Delta or Omicron BA.1/2 variants.

123 For the Delta wave, we focused on a subgroup of 797 participants from 196 households (Delta
124 wave subgroup, Table 1, Extended Data Fig. 1) who remained SARS-CoV-2 naïve or had a single
125 prior SARS-CoV-2 infection before the Delta wave (hence, removing vaccinated and repeatedly
126 infected individuals from the analysis; see Fig. 1 for the timing of the Delta wave). We define prior
127 infection as positivity on the Roche Elecsys anti-nucleocapsid assay (an assay was optimized to
128 detect prior infection [33]), and/or rRT-PCR-positivity, at or before blood draw 5 (refer to BD5
129 hereafter). SARS-CoV-2 infections during the Delta wave were inferred based on the anti-
130 nucleocapsid antibody level of two pre- and one post- Delta wave serum samples, as previously
131 described [30]. We focused on households with no more than six infected household members during
132 this wave, due to computational constraints of the transmission model (see Methods for details).
133 Among the 797 subgroup participants, 34% (273/797) were infected during the Delta wave, with
134 attack rates of 42% (229/544) and 17% (44/253) for naïve and previously infected participants,
135 respectively.

136 To identify CoPs against the Delta variant, for the 253 participants who had been previously
137 infected, we measured their anti-D614G nAb titers (measured as the inhibitory dilution at which
138 50% neutralization is attained, referred to as $ID_{50}$ hereafter), using the blood draw immediately
139 preceding the Delta wave (BD5). To evaluate the potential impact of antibody waning, we also
140 measured the peak nAb level for each participant (defined as the highest anti-D614G nAb titer
141 among the first 5 blood draws). We then calculated the degree to which nAbs had waned from
142 peak level to that at BD5 by calculating the difference between peak nAb titer and nAb titer at
143 BD5 (denoted as $\Delta nAb^W$ hereafter). If the peak response was already below the nAb assay
144 detection threshold (which is set at 20), then $\Delta nAb^W$ was also assigned to be below the threshold,

since further titer drop was not detectable. Notably, 28% (32/113) and 58% (81/140) of individuals previously infected with D614G and Beta exhibited anti-D614G nAb titers below the detection threshold at BD5, respectively (Extended Data Table 1). The proportion below the detection threshold was higher for individuals previously infected with the Beta variant than the D614G variant, given the Beta variant has eight amino acid difference in the spike, resulting in an antigenically distinct receptor binding domain compared to the D614G variant used in the neutralization assay. However, more than 90% of individuals remained positive on the Roche Elecsys anti-nucleocapsid assay for both prior D614G and Beta exposed individuals [33], despite low nAb titer level (Extended Data Table 1).

Fig. 2a shows the Delta wave participants anti-D614G nAb titers at peak and at BD5. The $ID_{50}$ geometric mean titer (GMT) was 125 (95% CI 97 – 161) at peak and waned to 85 (95% CI 69 – 104) at BD5, representing an average 1.47 (95% CI 1.32 – 1.67) fold reduction due to waning. The anti-D614G nAb titers (in log scale) at peak and at BD 5 were highly correlated (Pearson correlation coefficient 0.89, $p<0.0001$). Comparing the nAb titers between individuals who were infected during the Delta wave vs. those who were not infected, we found that the GMTs of infected individuals was significantly lower than that of uninfected individuals for both anti-D614G nAb at peak level and at BD5 (Fig. 2b-c). In contrast, we did not find a significant difference in the degree of antibody loss due to waning ($\Delta nAb^{W}$) between infected and uninfected individuals (Fig. 2d).

Similarly, for the Omicron wave, we focused on a subgroup of 535 participants from 184 households who had only one prior SARS-CoV-2 infection (vaccinated and repeatedly infected individuals were removed from the analysis) or remained naïve just before the Omicron wave (see Table 1 and Extended Data Fig. 2 for a description of participants and Fig. 1 for the timing of the Omicron wave). Prior SARS-CoV-2 infection was ascertained in a similar fashion as for the Delta wave (i.e., positivity by anti-nucleocapsid assay and/or rRT-PCR for the first 8 blood draws). Infections during the Omicron wave were inferred based on the anti-nucleocapsid antibody level of two pre- and one post- Omicron wave serum samples, as previously described [30]. Two thirds, or 67% (359/535), of participants included in the Omicron BA.1/2 wave analysis were infected by

these variants, with attack rates of 77% (149/193) and 61% (210/342) for naïve and previously infected individuals, respectively.

To evaluate nAbs as CoP in the context of Omicron's extensive immune escape, we measured both the anti-D614G nAb titers and anti-Omicron BA.1 nAb titers for serum samples collected at blood draw 8 (the blood draw taken shortly before the onset of the Omicron wave, referred to as BD8 hereafter). Given that none of the participants had been infected by Omicron prior to BD8, the anti-Omicron BA.1 neutralizing activity at this time point originated from cross-reactive antibodies elicited by prior variant infections. Thus, the difference between anti-D614G and anti-BA.1 nAb titers at BD8 represents the quantity of anti-D614G nAbs that failed to recognize mutated epitopes on Omicron BA.1, resulting in a lack of neutralizing function against Omicron BA.1. For the remainder of the manuscript, we will use $\Delta nAb^E$ to represent the quantity of antibodies able to neutralize D614G but not Omicron BA.1 due to mutations in the Omicron spike. Similarly to the Delta wave subgroup, a significant proportion of previously infected individuals in the Omicron wave subgroup exhibited anti-D614G and anti-Omicron nAb titers below the detection threshold at BD8 (Extended Data Table 1). The absence of detectable nAbs was also more pronounced when the variant causing prior exposure and the spike used in the neutralization assay were mismatched. (Extended Data Table 1). Roche Elecsys anti-nucleocapsid assay remained robust in detecting prior infection [33], despite low nAb titer level (Extended Data Table 1).

Fig. 2e shows the anti-D614G and the anti-BA.1 nAb titers at BD8 for participants included in the Omicron wave analysis. The nAb GMT against D614G was 122 (95% CI 103 – 145) and 30 (95% CI 27 – 34) for antibodies that could neutralize BA.1, representing an average 4.01 (95% CI 3.53 – 4.58) -fold reduction attributed to the immune evasive properties of Omicron. The anti-D614G and anti-BA.1 nAb titers (in log scale) at BD 8 were modestly correlated (Pearson correlation coefficient 0.64, $p<0.0001$). Comparing the nAb titers between individuals who were infected during the Omicron wave vs. those who were not infected, we did not find significant differences in GMT levels for anti-D614G nAb, anti-BA.1 nAb, or $\Delta nAb^E$ (Fig. f-h). However, it

200 is worth noting that the point estimates of GMTs were higher for uninfected individuals compared
201 to infected individuals across all three measurements.

202

203 **Pre-exposure nAb titer as CoP against variant infection**

204 We conducted mediation analyses in a household transmission modelling framework to investigate
205 how nAb titers against SARS-CoV-2 variants at the onset of a SARS-CoV-2 wave mediate the
206 risk of infection during the corresponding epidemic wave [34,35]. Specifically, following the causal
207 inference framework proposed by Halloran and Struchiner [36], we introduced SARS-CoV-2
208 transmission probabilities as causal parameters, representing either the risk of acquiring infection
209 from the general community or the per-contact transmission risk within the household.
210 Transmission probabilities were dependent on an individual's prior infection history, the level of
211 pre-existing nAb titers (mediators), and other confounding factors (age, gender, comorbidities).
212 We fitted a chain-binomial household transmission model, parametrized by the transmission
213 probabilities, to the infection outcomes of the Delta and Omicron waves among all subgroup
214 participants and evaluated how the level of nAb titers mediated SARS-CoV-2 transmission
215 probability. The details of the mediation analysis are described in the Methods.

216 For the Delta wave mediation analysis, we considered anti-D614G nAb titer at BD5 as candidate
217 mediator of protection and the quantity of antibodies that had waned from peak ($\Delta nAb^{W}$) as
218 putative negative control (i.e., we hypothesize that antibodies lost due to waning could not
219 conceivably contribute to protection). For the Omicron wave, we considered anti-BA.1 nAb titer
220 at BD8 as candidate mediator of protection and the quantity of nAbs that escape Omicron
221 neutralization ($\Delta nAb^{E}$) at BD8 as putative negative control. We used the term "direct effect" from
222 the causal inference framework to refer to the effect of exposure (prior infection) on the outcome
223 (repeat infection during the Delta or Omicron wave) absent the mediators (nAb titers). Conversely,
224 the term "indirect effect" represents the effect of exposure (prior infection) on the outcome (repeat
225 infection) that operates through the mediators (nAb titers). We estimated both the direct effect of
226 prior infection and effects mediated through specific nAb titers against serologically confirmed
227 SARS-CoV-2 infections. We report the estimates of the mediation analysis for both Delta and
228 Omicron wave in Table 2. For the ease of interpretation, we then translate the estimated odds ratios

229 into risk reductions (1 – odds ratio), along with other estimates in causal diagrams depicted in Fig.
230 3.

231 Our findings indicate that immunity derived from prior infection, overall, reduced the risk of
232 contracting a Delta wave infection by 61% (95%CI: 59% – 63%) (Fig 3a). Notably, nAbs
233 represented an important mediator of this overall protection: for every 10-fold increase in the anti-
234 D614G nAb titers at BD5, the risk of infection decreased by 40% (95% CI 19% – 56%). In contrast,
235 the decline in nAbs from peak levels to BD5 ($\Delta nAb^{W}$) showed no contribution to the overall
236 protection, with a risk reduction per 10-fold increase of -1% (95%CI: -21% – 16%). This result
237 indicated that waning of neutralizing antibodies results in waning of protection, in agreement with
238 our hypothesis. Furthermore, we estimated that the protection mediated through anti-D614G nAbs
239 at BD5 accounted for 37% (95% CI: 34% - 40%) of the overall protection derived from prior
240 infection, suggesting that over half of the protection against Delta was not mediated by serum nAbs
241 against D614G. Lastly, our analysis indicated that individuals reinfected with the Delta variant
242 were 78% (95% CI: 24% – 94%) less likely to transmit the infection to other household members
243 compared to those who experienced primary infections (Fig. 3a). This finding suggested that even
244 in cases where prior immunity is not sufficient to block reinfection with the Delta variant,
245 infection-induced immunity still offered sizable mitigation against onward transmission.

246 The causal diagram depicting the mediation analysis for the Omicron wave is illustrated in Fig.
247 3b. Our findings indicate that, overall, prior infection-derived immunity resulted in a 37% (95%CI:
248 35% – 38%) reduction in the risk of contracting an Omicron wave infection, a notably lower effect
249 compared to that of the Delta wave. We observed that, anti-Omicron nAbs at BD8 significantly
250 mediated protection against the Omicron BA.1/2 variants: for every 10-fold increase in anti-
251 Omicron nAb titers, the risk of Omicron BA.1/2 infection decreased by 28% (95% CI: 6% – 44%).
252 Conversely, antibodies unable to neutralize Omicron due to immune escape ($\Delta nAb^{E}$) did not
253 mediate protection against Omicron BA.1/2 infection, with risk reduction of -1% (95% CI: -21%
254 – 16%) per 10-fold titer increase. Furthermore, we estimated that the protection mediated through
255 anti-BA.1 nAbs at BD8 accounted for only 11% (95% CI: 9% - 12%) of the total protection
256 conferred by prior exposure. This, coupled with the observation that Omicron BA.1 caused an
257 average of 4.01-fold drop in nAb titers (Fig. 2e), underscores Omicron BA.1/2's ability to evade
258 host protective immunity mediated through nAbs. Additionally, in contrast to the Delta wave,

individuals reinfected with the Omicron variant were as likely to transmit the infection to other household members compared to those who experienced primary infections (risk reduction: -17%, (95% CI: -110% − 35%)). These observations suggested that Omicron not only evaded prior immunity's protection against acquisition of infection but also escaped protection against onward transmission.

Although neutralizing titers measured at BD5 and BD8 offered a temporally proximate evaluation of protective immunity preceding the onset of the Delta and Omicron waves, we could not identify the immune mediators responsible for the direct effects of prior immunity (i.e., the fraction of protection that was not mediated by nAbs) due to lack of additional serum biomarkers. We could however estimate the potential for these direct effects to wane over time. To do so, we modeled an exponential decline for the direct effect based on the time elapsed since prior infection and jointly estimated the duration of protection for both the Delta and Omicron waves' analysis. We found that protection not mediated by nAbs decreased with time, with a waning half-life of 121 (95%CI: 72 − 242) days (Fig. 3, Table 2). After adjusting for waning, the effect sizes of protection from direct effects were similar for both variants, with odds ratios of acquiring infection (compared to naïve individuals) of 0.34 (95% CI: 0.17, 0.68) and 0.29 (95% CI: 0.17, 0.50) for the Delta and Omicron wave, respectively, in the absence of waning (Table 2). These results suggested that, while Omicron escaped pre-existing neutralizing antibodies, protection from other immune effectors was preserved against this variant. The waning half-life of protection not mediated by nAbs was estimated at approximately 4 months in our study, comparable to the reported waning timescale of T-cell immunity [37,38]. Several sensitivity analyses demonstrating the robustness of the findings of the mediation analysis were reported in the Methods.

## Discussion

In this cohort of unvaccinated individuals, we found that nAb titers immediately before the onset of the Delta wave (i.e., anti-D614G nAb level at BD5) correlated with protection against Delta wave infections. Moreover, we demonstrated that nAb titers lost over time due to waning (i.e., $\Delta nAb^{W}$) were not associated with protection, aligning with the expectation that waning of nAbs in serum corresponds to waning of clinical protection. For the Omicron wave subgroup, we further

289 investigated the impact of immune escape against protection mediated through nAbs. We found
290 that only anti-Omicron BA.1 nAbs correlated with protection against infection during the Omicron
291 BA.1/2 wave, whereas anti-D614G nAbs that were unable to neutralize Omicron BA.1 due to spike
292 escape mutations did not protect. This indicated that antibodies capable of neutralizing D614G but
293 not Omicron BA.1 *in vitro* translates to a diminished protection against Omicron BA.1/2 infection
294 among PHIRST-C participants. The identification of variant-neutralizing antibodies derived from
295 infection-induced immunity as CoPs against infections for both Delta and Omicron variants aligns
296 with findings from studies on variant-specific correlates for vaccine-induced or hybrid immunity
297 [21–24]. Considering that antibody-mediated protection against acquisition of infection likely operates
298 at the mucosal site rather than in serum, it is interesting that serum antibodies levels can anticipate
299 protection [26]. In a recent analysis of the data from the COVE trial, Zhang et. al. further
300 demonstrated that boosting of nAb titers against Omicron by a third dose of mRNA-1273 vaccine,
301 afforded additional protection against Omicron compared to individuals who only received 2 doses
302 of the mRNA-1273 vaccine. [22] Collectively, these empirical data lend support for using nAbs
303 against circulating variant as immuno-bridging markers for periodic vaccine updates.

304 While a comprehensive understanding of the role of nAbs in SARS-CoV-2 protection is
305 important, a key finding of our study is that nAb titers did not fully mediate protection conferred
306 by prior infection. In the case of the Delta wave subgroup, we estimate that anti-D614G nAbs
307 mediate 37% of protection, a proportion comparable to vaccine-induced nAbs [15]. In contrast, for
308 the Omicron BA.1/2 wave subgroup, anti-Omicron BA.1 nAbs are estimated to mediate only 11%
309 of protection, which was substantially lower than that observed for the Delta wave. This low
310 percentage of protection mediated by nAbs for the Omicron BA.1/2 wave could be attributed to
311 the highly immune evasive nature of Omicron against neutralizing activity. Omicron effectively
312 rendered a significant proportion of serum anti-D614G nAbs nonfunctional against Omicron. The
313 large proportion of overall protection that was not mediated by nAbs could be explained by a
314 variety of immune mechanisms, including the Fc-effector function of binding antibodies, and T-
315 cell functions, both of which are resilient against mutations in VOCs [14,39]. Additionally, SARS-
316 CoV-2 initially infects and predominantly transmits through the upper respiratory tract. Mucosal
317 immunity in the upper respiratory tract therefore likely plays a key role in preventing SARS-CoV-
318 2 infection, and may not be fully represented by immune markers in serum [40]. Our study validates
319 the use of serum nAbs as CoP against reinfection but also suggests potential important roles for

other candidate functions that could act as "co-correlates" of protection [41]. This is particularly important because these mechanisms may be more broadly cross-protective against future variants than neutralizing antibodies. Future CoP analyses incorporating measurements of T-cell immunity and non-neutralizing antibody functions, ideally at the mucosal site, could potentially disentangle these important protective mechanisms and inform design of next generation vaccines [26,42–44].

Our study has several limitations. Firstly, the vaccination rate in the PHIRST-C cohort was low at the time of the analysis; with <20% participants fully vaccinated prior to the Omicron BA.1/2 wave (thus excluded from our analysis). Consequently, we lacked sufficient statistical power to assess CoPs for vaccine-induced (or hybrid) immunity and compare with our findings for infection-induced immunity in the same cohort. Secondly, we focused on SARS-CoV-2 infections that were ascertained by seroconversion or amnestic boosting of the anti-nucleocapsid antibodies. However, not all PCR-positive SARS-CoV-2 infections led to systemic antibody response [30,45,46]. Thus, our CoP analysis does not account for protection against abortive or transient infections that do not lead to systemic antibody responses. We also could not evaluate CoPs against symptomatic cases, as there was no systemic monitoring of SARS-CoV-2 symptoms for the cohort population during the Omicron BA.1/2 wave. Further, severe outcomes (hospitalizations and deaths) due to SARS-CoV-2 infections were rare throughout the course of the PHIRST-C study and evaluation of protection against those outcomes is under-powered. Understanding protection against severe outcomes is important from both clinical and public health prospective, thus warranting further studies. Thirdly, the strains of antigens used in neutralization assay were not perfectly matched to the circulating variants in the CoP analysis. For the Delta wave analysis, we evaluated anti-D614G antibody titers (rather than anti-Delta titers). Although Delta is not as immune evasive as Omicron with respect to D614G, there are substitutions on the spike of Delta (i.e., L452R, T478K) that are linked to moderate antigenic escape [47,48]. In addition, though infections were predominantly caused by the Delta variant during the Delta wave epidemic, other variants also circulated at low levels during the same time period, including Alpha and C.1.2 [30]. Similarly, genomic surveillance revealed that while Omicron BA.1 accounted for the majority of infections during the Omicron wave, Omicron BA.2 also co-circulated, with potential antigenic spike substitutions (e.g., T376A, D405N, R408S) that were not present in BA.1 [30,48,49]. Thus, using a BA.1-specific neutralizing assay may introduce bias in our CoP analysis, particularly against Omicron BA.2. Lastly, we only measured serum antibodies, but did not have any information on antibody response at the mucosal

site or on cell-mediated immunity. While serum IgG nAbs may transudate into the nasal mucosa and thereby play a role in protection, the contribution of locally produced nasal IgA nAb remains to be investigated.

Moving forward, future works focusing on understanding how protective immunity accumulates through repeated infections, vaccinations, and hybrid immunity, and identifying a suite of predictive markers of protection reflecting different arms of immune responses, are key to anticipating long-term SARS-CoV-2 burden, optimizing vaccine boosters, and designing next generation SARS-CoV-2 vaccines.

## Acknowledgment

We are thankful to all the participants who kindly agreed to take part in the study, as well as to the PHIRST group. We are grateful to Professor Benjamin J. Cowling and Professor M. Elizabeth Halloran for their insightful feedback on the paper. We deeply appreciate the three anonymous reviewers for their constructive review of the paper. The findings and conclusions in this report are those of the authors and do not necessarily represent the official position of the NIH or the U.S. Centers for Disease Control and Prevention. **Funding:** This work was supported by the National Institute for Communicable Diseases of the National Health Laboratory Service and the U.S. Centers for Disease Control and Prevention [cooperative agreement number: 6 U01IP001048] and Wellcome Trust (grant number 221003/Z/20/Z) in collaboration with the Foreign, Commonwealth and Development Office, United Kingdom. PLM and JNB are supported by the Bill and Melinda Gates Foundation through the Global Immunology and Immune Sequencing for Epidemic Response (GIISER) program (INV-030570) and receive funding from the Wellcome Trust (226137/Z/22/Z). PLM is supported by the South African Research Chairs Initiative of the Department of Science and Innovation and National Research Foundation of South Africa and the SA Medical Research Council SHIP program.

## Author Contributions Statement

KS, JNB, ST, JK, AvG, MLM, NW, JM, NAM, KK, LL, CV, PLM, CC designed the experiments. JNB, CC, JK, PLM and ST accessed and verified the underlying data. JNB, ST, JK, VSM, QM,

HK, AvG, MLM, NW, JM, MC, NAM, KK, LL, JdT, TM, PLM, CC collected the data and performed laboratory experiments. KS, JNB, ST, JK, AvG, MLM, NW, JM, MC, NAM, KK, LL, JdT, TM, CV, and CC analyzed the data and interpreted the results. KS, JNB, CV, PLM, and CC drafted the manuscript. All authors critically reviewed the article. All authors had access to all the data reported in the study.

## Competing Interests Statement

CC has received grant support from Sanofi Pasteur, US CDC, the Bill & Melinda Gates Foundation, the Taskforce for Global Health, Wellcome Trust and the South African Medical Research Council. AvG has received grant support from Sanofi Pasteur, Pfizer related to pneumococcal vaccine, CDC and the Bill & Melinda Gates Foundation. NW reports grants from Sanofi Pasteur and the Bill & Melinda Gates Foundation. NAM has received a grant to his institution from Pfizer to conduct research in patients with pneumonia and from Roche to collect specimens to assess a novel TB assay. JM has received grant support from Sanofi Pasteur. The remaining authors declare no competing interests

## Consortia Authorship

The PHIRST-C group: Jinal N. Bhiman[2,3], Amelia Buys[4], Maimuna Carrim[4,7], Cheryl Cohen[4,5], Linda de Gouveia[4], Mignon du Plessis[4,7], Jacques du Toit[11], Francesc Xavier Gómez-Olivé[11], Kathleen Kahn[11], Kgaugelo Patricia Kgasago[9], Jackie Kleynhans[4,5], Retshidisitswe Kotane[4], Limakatso Lebina[9], Neil A Martinson[9,10], Meredith L McMorrow[6,8], Tumelo Moloantoa[4], Jocelyn Moyes[4,5], Stefano Tempia[4,5,6], Stephen Tollman[11], Anne von Gottberg[4,7], Floidy Wafawanaka[11], Nicole Wolter[4,7]

401 # Tables:

402 **Table 1: Characteristics of the PHIRST-C cohort's Delta wave subgroup and Omicron wave subgroup**
403 **populations, respectively.** *PLWH: people living with HIV. **Here it indicates if a participant of the Delta/Omicron
404 wave subgroup was infected (either primary or repeat infection) during the Delta/Omicron BA.1 wave.

| | **Delta wave subgroup 196 households** | **Omicron wave subgroup 184 households** |
|---|---|---|
| **Characteristics** | Number of individuals (%) | Number of individuals (%) |
| All | 797 (100) | 535 (100) |
| **Study site** | | |
| Rural | 427 (54) | 300 (56) |
| Urban | 370 (46) | 235 (44) |
| **Age group, in years** | | |
| 0-4 | 90 (11) | 77 (14) |
| 5-12 | 270 (34) | 231 (43) |
| 13-18 | 111 (14) | 80 (15) |
| 19-34 | 126 (16) | 84 (16) |
| 35-59 | 126 (16) | 43 (8) |
| 60+ | 74 (9) | 20 (4) |
| **Sex** | | |
| Male | 324 (41) | 229 (43) |
| Female | 473 (59) | 306 (57) |
| **Household size** | | |
| 3-5 | 372 (47) | 254 (48) |
| 6-8 | 264 (33) | 197 (37) |
| 9-12 | 124 (15) | 72 (13) |
| 13+ | 37 (5) | 12 (2) |
| **HIV status** | | |
| Negative | 673 (85) | 496 (93) |
| PLWH* | 97 (12) | 31 (6) |
| Unknown | 27 (3) | 8 (1) |
| **Prior immunity** | | |
| Naive | 544 (68) | 193 (36) |
| Previously infected | 253 (32) | 342 (64) |
| Variant of prior infection: | | |
| D614G | 113 (14) | 61 (11) |
| Beta | 140 (18) | 120 (22) |
| Delta | – | 161 (31) |
| **Infected**** | | |
| Yes | 273 (34) | 359 (67) |
| No | 524 (66) | 176 (33) |

**Table 2: Mediation analysis for nAbs as CoPs against Delta and Omicron wave infections, with a waning model for direct effect.** Average and 95% CIs are provided for each of the model parameters. $\Delta nAb^{W}$: the quantity of anti-D614G nAbs waned from peak level to that at BD5. $\Delta nAb^{E}$: the quantity of antibodies that can neutralize D614G but fail to neutralize Omicron BA.1 at BD8 due to Omicron's immune escape.

| **Wave** | | | Delta | Omicron |
|---|---|---|---|---|
| **Protection against reinfection** | **Direct effect** (Protection absent of nAbs) | **Effect size** (odds ratio, absent of waning) | 0.34 (0.17, 0.68) | 0.29 (0.17, 0.50) |
| | | **Waning half-life** (days) | 121 (72, 242) | |
| | **Mediators effect** (Protection from nAbs) | **Anti-D614G nAb** (odds ratio, per 10-fold increase) | 0.60 (0.44, 0.81) | – |
| | | $\boldsymbol{\Delta nAb^{W}}$ (odds ratio, per 10-fold increase) | 1.01 (0.74, 1.37) | – |
| | | **Anti-Omicron BA.1 nAb** (odds ratio, per 10-fold increase) | – | 0.72 (0.56, 0.94) |
| | | $\boldsymbol{\Delta nAb^{E}}$ (odds ratio, per 10-fold increase) | – | 1.01 (0.84, 1.21) |
| | **Total protection** (relative risk compared to naïve individuals) | | 0.39 (0.37, 0.41) | 0.63 (0.62, 0.65) |
| | **Proportion of protection mediated by nAbs** | | 37% (34%, 40%) | 11% (9%, 12%) |
| **Protection against onward transmission** (Odds ratio compared to naïve individuals) | | | 0.22 (0.06, 0.76) | 1.17 (0.65, 2.10) |

# Figures:

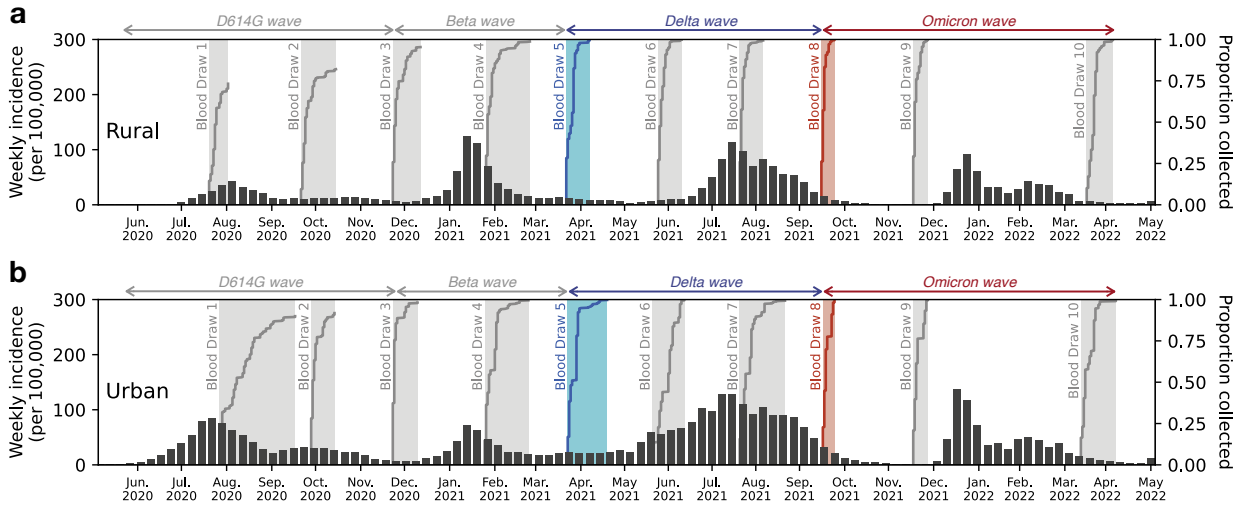


**Fig. 1: Timing of cohort sample collections with respect to SARS-CoV-2 variants' circulations in the two study sites. a**, Timing of the blood draws with respect to the SARS-CoV-2 epidemic waves in the rural site (Agincourt) of the PHIRST-C cohort. Bar plot represents the weekly incidence (per 100,000 population) of SARS-CoV-2 cases from routine surveillance data collected in Ehlanzeni District, Mpumalanga Province (where rural participants reside). The shaded areas represent the timing of the serum sample collections for the 10 blood draws. Each curve within the shaded area indicates the cumulative proportion of participants' serum samples collected over time. The Delta wave subgroup analysis focuses on nAb titers among serum samples collected during blood draw 5 (blue shade); the Omicron BA.1 wave analysis focuses on nAb titers among serum samples collected during blood draw 8 (red shade). **b**, Same as (A), but for the urban site (Klerksdorp). The routine surveillance data (bar plot) were collected from Dr. Kenneth Kaunda District, North West Province (where urban participants reside).

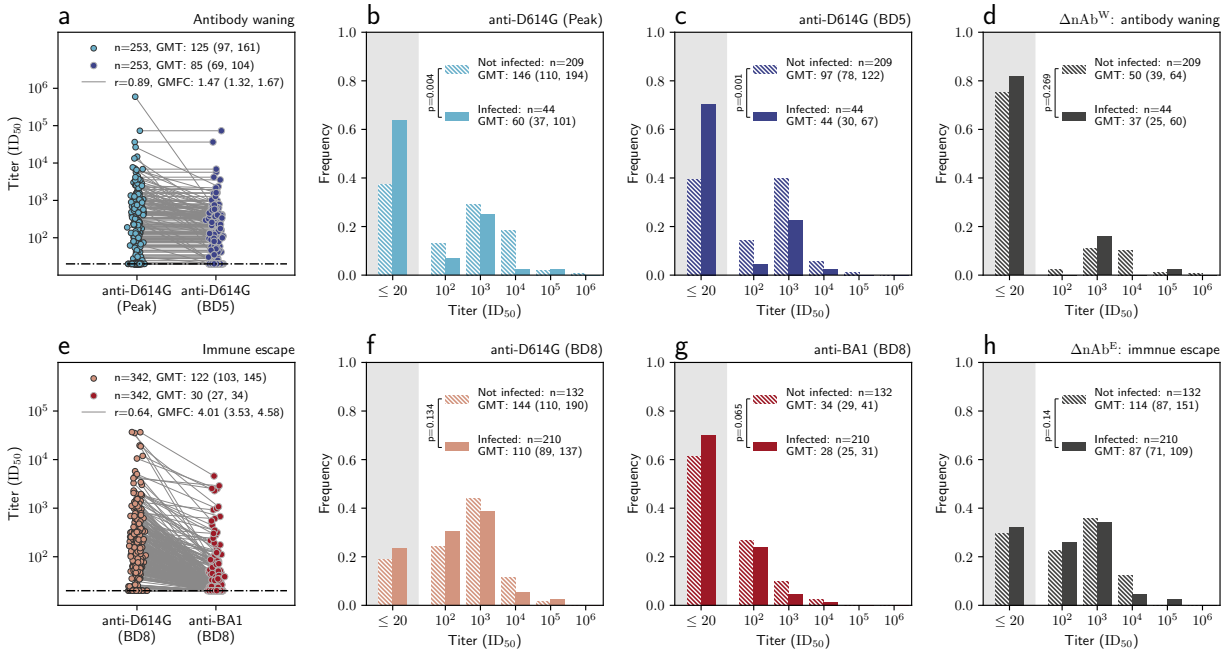


**Fig. 2: Anti-D614G and anti-BA.1 nAb titers for the Delta wave and the Omicron wave analysis. a**, for Delta wave subgroup, the distribution of the peak anti-D614G nAb titer up to BD5 (light blue dots) and the anti-D614G nAb titer at BD5 (dark blue dots), among individuals who had one prior SARS-CoV-2 infection before blood draw 5. Each dot represents one individual, with two measurements of the same individual connected through a gray line. GMFC: geometric fold change from peak anti-D614G titer to that at BD5; GMT: geometric mean titer; r: Pearson correlation coefficient. **b**, for Delta wave subgroup, the distribution of the peak anti-D614G nAb titer up to BD5, stratified by individuals who were infected during the Delta wave (solid bar) vs those who were not infected (dashed bar). Independent samples t-test (two-sided) is used to determine the statistical significance (p-value reported on the legend) of difference between the GMT of the two groups. **c**, same as **b** but for anti-D614G nAb titers at BD5. **d**, same as **b** but for $\Delta nAb^W$ (defined as the difference between anti-D614G titers at peak and at BD5). **e**, for Omicron wave subgroup, the distribution of anti-D614G nAb titers (light red dots) and anti-BA.1 titers at BD8 (dark red dots), among individuals who had one prior SARS-CoV-2 infection before BD8. Each dot represents one individual, with two measurements of the same individual connected through a gray line. **f**, for the Omicron wave subgroup, the distribution of the anti-D614G nAb titer at BD5, stratified by individuals who were infected during the Omicron wave (solid bar) vs those who were not infected (dashed bar). Independent samples t-test (two-sided) is used to determine the statistical significance (p-value reported on the legend) of difference between the GMT of the two groups. **g**, same as **f** but for anti-BA.1 nAb titers at BD8. **d**, same as **f** but for $\Delta nAb^E$ (defined as the difference between anti-BA.1 and anti-D614G titers at BD8).

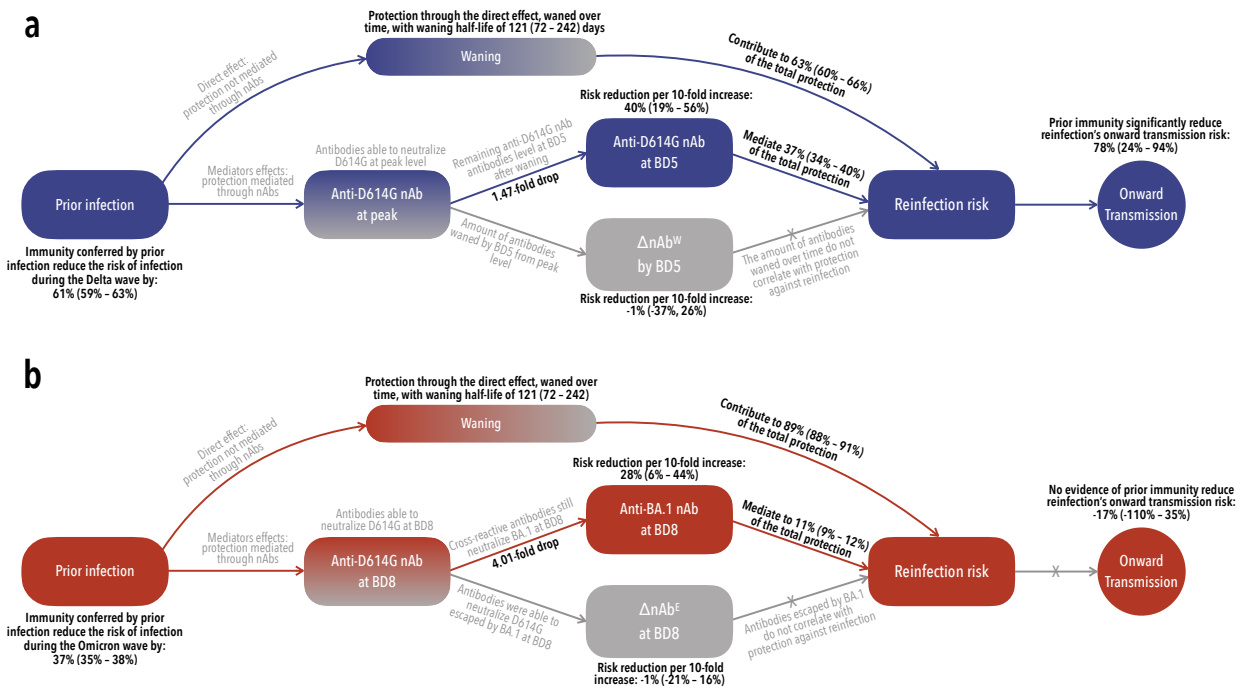


**Figure 3: Causal diagrams for the mediation analyses. a:** Causal diagram of the Delta wave mediation analysis showing the hypothesized relationship between prior immunity (induced by prior SARS-CoV-2 infection) and SARS-CoV-2 infection (outcome of interest) during Delta wave. The mediators of interest are anti-D614G nAbs at BD5 and $\Delta nAb^{W}$ (the quantity of anti-D614G nAbs waned from peak level to that at BD5). The direct effect represents protection operating through immune mechanisms other than the mediators of interest. We hypothesize that the direct effect could wane over time since the initial immune exposure. For the prospective cohort data, both mediator-outcome confounding and exposure-outcome confounding factors need to be adjusted for in the mediation analysis, as the immune exposure (prior SARS-CoV-2 infection) was not randomly assigned (unlike SARS-CoV-2 randomized-control vaccine trials where vaccination was randomly assigned to the participants). Furthermore, cohort participants may experience heterogenous levels of SARS-CoV-2 exposure due to different intensity SARS-CoV-2 transmission in their household settings. We adjust this by embedding the mediation analysis in a mechanistic household transmission model (detailed in Methods). We also look at the impact of prior immunity on the reduction of onward transmission, conditional on the failure of preventing reinfection. The estimates of the Delta wave mediation analysis are presented in Table 2. **b:** Same as a but for the Omicron wave analysis. The mediators of interest are anti-BA.1 nAbs at BD8 and $\Delta nAb^{E}$ (the quantity of antibodies that can neutralize D614G but fail to neutralize Omicron BA.1 at BD8 due to Omicron's immune escape.). The estimates of the Omicron wave mediation analysis are presented in Table 2.

463 **Reference:**


464 1. Statement on the fifteenth meeting of the IHR (2005) Emergency Committee on the
465 COVID-19 pandemic. https://www.who.int/news/item/05-05-2023-statement-on-the-
466 fifteenth-meeting-of-the-international-health-regulations-(2005)-emergency-committee-
467 regarding-the-coronavirus-disease-(covid-19)-pandemic.
468 2. WHO Coronavirus (COVID-19) Dashboard. https://covid19.who.int/.
469 3. WHO – COVID19 Vaccine Tracker. https://covid19.trackvaccines.org/agency/who/.
470 4. Watson, O. J. *et al.* Global impact of the first year of COVID-19 vaccination: a
471 mathematical modelling study. *Lancet Infect. Dis.* **22**, 1293–1302 (2022).
472 5. Gozzi, N. *et al.* Estimating the impact of COVID-19 vaccine inequities: a modeling study.
473 *Nat. Commun.* **14**, 3272 (2023).
474 6. Wang, Q. *et al.* Mapping global acceptance and uptake of COVID-19 vaccination: A
475 systematic review and meta-analysis. *Commun. Med.* **2**, 113 (2022).
476 7. Lazarus, J. V. *et al.* A survey of COVID-19 vaccine acceptance across 23 countries in 2022.
477 *Nat. Med.* **29**, 366–375 (2023).
478 8. Bergeri, I. *et al.* Global SARS-CoV-2 seroprevalence from January 2020 to April 2022: A
479 systematic review and meta-analysis of standardized population-based studies. *PLoS Med.*
480 **19**, e1004107 (2022).
481 9. Lewis, H. C. *et al.* SARS-CoV-2 infection in Africa: a systematic review and meta-analysis
482 of standardised seroprevalence studies, from January 2020 to December 2021. *BMJ Glob*
483 *Health* **7**, (2022).
484 10. Wang, Q. *et al.* Antibody evasion by SARS-CoV-2 Omicron subvariants BA.2.12.1, BA.4
485 and BA.5. *Nature* **608**, 603–608 (2022).

486 11. Ito, J. *et al.* Convergent evolution of SARS-CoV-2 Omicron subvariants leading to the
487 emergence of BQ.1.1 variant. *Nat. Commun.* **14**, 2671 (2023).
488 12. Cao, Y. *et al.* BA.2.12.1, BA.4 and BA.5 escape antibodies elicited by Omicron infection.
489 *Nature* **608**, 593–602 (2022).
490 13. Cao, Y. *et al.* Imprinted SARS-CoV-2 humoral immunity induces convergent Omicron RBD
491 evolution. *Nature* **614**, 521–529 (2023).
492 14. Goldblatt, D., Alter, G., Crotty, S. & Plotkin, S. A. Correlates of protection against SARS-
493 CoV-2 infection and COVID-19 disease. *Immunol. Rev.* **310**, 6–26 (2022).
494 15. Gilbert, P. B. *et al.* Immune correlates analysis of the mRNA-1273 COVID-19 vaccine
495 efficacy clinical trial. *Science* **375**, 43–50 (2022).
496 16. Fong, Y. *et al.* Immune correlates analysis of the PREVENT-19 COVID-19 vaccine efficacy
497 clinical trial. *Nat. Commun.* **14**, 331 (2023).
498 17. Fong, Y. *et al.* Immune correlates analysis of the ENSEMBLE single Ad26.COV2.S dose
499 vaccine efficacy clinical trial. *Nat Microbiol* **7**, 1996–2010 (2022).
500 18. Feng, S. *et al.* Correlates of protection against symptomatic and asymptomatic SARS-CoV-
501 2 infection. *Nat. Med.* **27**, 2032–2040 (2021).
502 19. Khoury, D. S. *et al.* Neutralizing antibody levels are highly predictive of immune protection
503 from symptomatic SARS-CoV-2 infection. *Nat. Med.* **27**, 1205–1211 (2021).
504 20. Earle, K. A. *et al.* Evidence for antibody as a protective correlate for COVID-19 vaccines.
505 *Vaccine* **39**, 4423–4428 (2021).
506 21. Atti, A. *et al.* Antibody correlates of protection against Delta infection after vaccination: A
507 nested case-control within the UK-based SIREN study. *J. Infect.* **87**, 420–427 (2023).

508 22. Zhang, B. *et al.* Omicron COVID-19 immune correlates analysis of a third dose of mRNA-
509 1273 in the COVE trial. *bioRxiv* (2023) doi:10.1101/2023.10.15.23295628.
510 23. Hertz, T. *et al.* Correlates of protection for booster doses of the SARS-CoV-2 vaccine
511 BNT162b2. *Nat. Commun.* **14**, 4575 (2023).
512 24. Gilboa, M. *et al.* Factors Associated With Protection From SARS-CoV-2 Omicron Variant
513 Infection and Disease Among Vaccinated Health Care Workers in Israel. *JAMA Netw Open*
514 **6**, e2314757 (2023).
515 25. Tang, J. *et al.* Respiratory mucosal immunity against SARS-CoV-2 after mRNA
516 vaccination. *Sci Immunol* **7**, eadd4853 (2022).
517 26. Knisely, J. M. *et al.* Mucosal vaccines for SARS-CoV-2: scientific gaps and opportunities-
518 workshop report. *NPJ Vaccines* **8**, 53 (2023).
519 27. Miyamoto, S. *et al.* Infectious virus shedding duration reflects secretory IgA antibody
520 response latency after SARS-CoV-2 infection. *Proc. Natl. Acad. Sci. U. S. A.* **120**,
521 e2314808120 (2023).
522 28. Markov, P. V. *et al.* The evolution of SARS-CoV-2. *Nat. Rev. Microbiol.* **21**, 361–379
523 (2023).
524 29. Cohen, C. *et al.* SARS-CoV-2 incidence, transmission, and reinfection in a rural and an
525 urban setting: results of the PHIRST-C cohort study, South Africa, 2020-21. *Lancet Infect.*
526 *Dis.* (2022) doi:10.1016/S1473-3099(22)00069-X.
527 30. Sun, K. *et al.* Rapidly shifting immunologic landscape and severity of SARS-CoV-2 in the
528 Omicron era in South Africa. *Nat. Commun.* **14**, 246 (2023).
529 31. Pulliam, J. R. C. *et al.* Increased risk of SARS-CoV-2 reinfection associated with emergence
530 of Omicron in South Africa. *Science* eabn4947 (2022).

531 32. Sun, K. *et al.* SARS-CoV-2 transmission, persistence of immunity, and estimates of
532 Omicron's impact in South African population cohorts. *Sci. Transl. Med.* eabo7081 (2022).
533 33. Elecsys® Anti-SARS-CoV-2. *Diagnostics*
534 https://diagnostics.roche.com/us/en/products/params/elecsys-anti-sars-cov-2.html.
535 34. Cowling, B. J. *et al.* Influenza hemagglutination-inhibition antibody titer as a mediator of
536 vaccine-induced protection for influenza B. *Clin. Infect. Dis.* **68**, 1713–1717 (2019).
537 35. Lim, W. W., Shuo, F., Wong, S.-S., Sullivan, S. G. & Cowling, B. J. Hemagglutination
538 inhibition antibody titers mediate influenza vaccine efficacy against symptomatic influenza
539 A(H1N1), A(H3N2), and B/Victoria infections. *J. Infect. Dis.* (2024)
540 doi:10.1093/infdis/jiae122.
541 36. Halloran, M. E. & Struchiner, C. J. Causal inference in infectious diseases. *Epidemiology* **6**,
542 142–151 (1995).
543 37. Cohen, K. W. *et al.* Longitudinal analysis shows durable and broad immune memory after
544 SARS-CoV-2 infection with persisting antibody responses and memory B and T cells. *Cell*
545 *Rep Med* **2**, 100354 (2021).
546 38. Dan, J. M. *et al.* Immunological memory to SARS-CoV-2 assessed for up to 8 months after
547 infection. *Science* **371**, (2021).
548 39. Eser, T. M. *et al.* Nucleocapsid-specific T cell responses associate with control of SARS-
549 CoV-2 in the upper airways before seroconversion. *Nat. Commun.* **14**, 2952 (2023).
550 40. Havervall, S. *et al.* Anti-Spike Mucosal IgA Protection against SARS-CoV-2 Omicron
551 Infection. *N. Engl. J. Med.* **387**, 1333–1336 (2022).
552 41. Plotkin, S. A. Vaccines: correlates of vaccine-induced immunity. *Clin. Infect. Dis.* **47**, 401–
553 409 (2008).

554 42. Morens, D. M., Taubenberger, J. K. & Fauci, A. S. Rethinking next-generation vaccines for
555 coronaviruses, influenzaviruses, and other respiratory viruses. *Cell Host Microbe* **31**, 146–
556 157 (2023).
557 43. Topol, E. J. & Iwasaki, A. Operation Nasal Vaccine-Lightning speed to counter COVID-19.
558 *Science immunology* vol. 7 eadd9947 (2022).
559 44. Fact Sheet: HHS Details $5 Billion 'Project NextGen' Initiative to Stay Ahead of COVID-
560 19. https://aspr.hhs.gov/newsroom/Pages/ProjectNextGen-May2023.aspx.
561 45. Liu, W. *et al.* Predictors of Nonseroconversion after SARS-CoV-2 Infection. *Emerg. Infect.*
562 *Dis.* **27**, 2454–2458 (2021).
563 46. Lindeboom, R. G. H. *et al.* Human SARS-CoV-2 challenge resolves local and systemic
564 response dynamics. *medRxiv* (2023) doi:10.1101/2023.04.13.23288227.
565 47. McCallum, M. *et al.* Molecular basis of immune evasion by the Delta and Kappa SARS-
566 CoV-2 variants. *Science* **374**, 1621–1626 (2021).
567 48. Wilks, S. H. *et al.* Mapping SARS-CoV-2 antigenic relationships and serological responses.
568 *Science* **382**, eadj0070 (2023).
569 49. Tegally, H. *et al.* Emergence of SARS-CoV-2 Omicron lineages BA.4 and BA.5 in South
570 Africa. *Nat. Med.* (2022) doi:10.1038/s41591-022-01911-2.
571 50. Wibmer, C. K. *et al.* SARS-CoV-2 501Y.V2 escapes neutralization by South African
572 COVID-19 donor plasma. *Nat. Med.* (2021) doi:10.1038/s41591-021-01285-x.
573 51. Netzl, A. *et al.* Analysis of SARS-CoV-2 Omicron Neutralization Data up to 2022-01-28.
574 *bioRxiv* 2021.12.31.474032 (2023) doi:10.1101/2021.12.31.474032.
575 52. Cox, D. R. Planning of experiments. **308**, (1958).

53. Imbens, G. W. & Rubin, D. B. *Causal Inference in Statistics, Social, and Biomedical Sciences*. (Cambridge University Press, 2015).

54. Longini, I. M., Jr & Koopman, J. S. Household and community transmission parameters from final distributions of infections in households. *Biometrics* **38**, 115–126 (1982).

55. Yang, Y., Longini, I. M., Jr, Halloran, M. E. & Obenchain, V. A hybrid EM and Monte Carlo EM algorithm and its application to analysis of transmission of infectious diseases. *Biometrics* **68**, 1238–1249 (2012).

585 # Methods

586 ## Ethics Statement

587 The PHIRST-C protocol was approved by the University of Witwatersrand Human Research Ethics
588 Committee (Reference 150808) and the U.S. Centers for Disease Control and Prevention's
589 Institutional Review Board relied on the local review (#6840). The protocol was registered on
590 clinicaltrials.gov on 6 August 2015 and updated on 30 December 2020
591 (https://clinicaltrials.gov/ct2/show/NCT02519803). Participants receive grocery store vouchers of
592 ZAR50 (USD 3) per visit to compensate for time required for specimen collection and interview.
593 All participants provided written informed consent for study participation. For minors, consent
594 was obtained from the parent or guardian.

595 ## Inferring Delta and Omicron wave infections based on longitudinal serum
596 samples.

597 We have previously described the serologic inference method for SARS-CoV-2 infections among
598 the PHIRST-C cohort participants during the Delta wave (3rd SARS-CoV-2 wave) and the Omicron
599 wave (4th SARS-CoV-2 wave) [30]. To briefly summarize, ascertainment of Delta wave infections
600 was based on the serial serologic readout of blood draws 5 and 6 (both before the Delta wave,
601 figure 1A-B), and 8 (post Delta wave), measured by the Roche Elecsys Anti-SARS-CoV-2
602 nucleocapsid assay [33]. The participants' serologic trajectories were then grouped into 13 categories
603 of distinct serum antibody patterns, reflecting the rise, waning, and/or amnestic boosting of anti-
604 nucleocapsid antibody levels. Because the Delta wave was also covered by intense virologic
605 sampling with twice-weekly nasopharyngeal swab collection, we grouped the 13 serologic
606 categories into indicators of either presence or absence of SARS-CoV-2 infection to achieve the
607 highest concordance with rRT-PCR-confirmed Delta infections. The Omicron wave was not
608 covered by the intense PCR testing; however, the timing of blood draws 8, 9, and 10 with respect
609 to the Omicron wave is similar to that of blood draws 5, 6, and 8 with respect to the Delta wave
610 (figure 1A-B). We thus apply the same classification method of serial serologic trajectories defined
611 by blood draws 8, 9, and 10 to infer SARS-CoV-2 infections during the Omicron BA.1/2 wave.

612 ## Laboratory Methods

613 **Serum nAb titers against SARS-CoV-2 D614G and BA.1 variants (Lentiviral Pseudovirus**
614 **Production and Neutralization Assay)**

615 Virus production and pseudovirus neutralization assays were done as previously described [50].
616 Briefly, 293T/ACE2.MF cells modified to overexpress human ACE2 (kindly provided by M.
617 Farzan (Scripps Research)) were cultured in DMEM (Gibco BRL Life Technologies) containing
618 10% heat-inactivated serum (FBS) and 3 μg $ml^{-1}$ puromycin at 37 °C, 5% $CO_2$. Cell monolayers
619 were disrupted at confluency by treatment with 0.25% trypsin in 1 mM EDTA (Gibco BRL Life
620 Technologies). The SARS-CoV-2, Wuhan-1 spike, cloned into pCDNA3.1 was mutated using the
621 QuikChange Lightning Site-Directed Mutagenesis kit (Agilent Technologies) and NEBuilder HiFi
622 DNA Assembly Master Mix (NEB) to include D614G (wild-type) or lineage defining mutations
623 for Delta (T19R, 156-157del, R158G, L452R, T478K, D614G, P681R and D950N) and ), Omicron
624 BA.1 (A67V, 69-70del, T95I, G142D, 143-145del, 211del, L212I, 214EPE, G339D, S371L, S373P,
625 S375F, K417N, N440K, G446S, S477N, T478K, E484A, Q493R, G496S, Q498R, N501Y, Y505H,
626 T547K, D614G, H655Y, N679K, P681H, N764K, D796Y, N856K, Q954H, N969K, L981F),
627 Omicron BA.2 (T19I, L24S, 25-27del, G142D, V213G, G339D, S371F, S373P, S375F, T376A,
628 D405N, R408S, K417N, N440K, S477N, T478K, E484A, Q493R, Q498R, N501Y, Y505H,
629 D614G, H655Y, N679K, P681H, N764K, D796Y, Q954H, N969K). Pseudoviruses were produced
630 by co-transfection in 293T/17 cells with a lentiviral backbone (HIV-1 pNL4.luc encoding the
631 firefly luciferase gene) and either of the full-length SARS-CoV-2 spike plasmids with PEIMAX
632 (Polysciences). Culture supernatants were clarified of cells by a 0.45μM filter and stored at −70 °C.
633 Plasma samples were heat-inactivated and clarified by centrifugation. Pseudovirus and serially
634 diluted plasma/sera were incubated for 1 h at 37 °C, 5% $CO_2$. Cells were added at $1 \times 10^4$ cells per
635 well after 72 h of incubation at 37 °C, 5% $CO_2$, luminescence was measured using PerkinElmer
636 Life Sciences Model Victor X luminometer. Neutralization was measured as described by a
637 reduction in luciferase gene expression after single-round infection of 293T/ACE2.MF cells with
638 spike-pseudotyped viruses. Titers were calculated as the reciprocal plasma dilution ($ID_{50}$) causing
639 50% reduction of relative light units.

640 Noting that we measured neutralization titer using a lentiviral-backboned pseudovirus
641 neutralization assay. A systematic review of Omicron neutralization data showed that pseudovirus
642 neutralization assays tend to report higher neutralizing titers compared to live-virus assays. The

643 titer drops from wild type to Omicron also tend to be less pronounced for pseudovirus platforms,
644 suggesting the pseudovirus assay may underestimate Omicron's capability to escape neutralization
645 [51].

646 **SARS-CoV-2 spike enzyme-linked immunosorbent assay (ELISA)**

647 For ELISA, Hexapro SARS-CoV-2 full spike protein with the D614G substitution was expressed
648 in Human Embryonic Kidney (HEK) 293F suspension cells by transfecting the cells with the
649 respective expression plasmid. After incubating for 6 days at 37°C, proteins were first purified
650 using a nickel resin followed by size exclusion chromatography. Relevant fractions were collected
651 and frozen at -80°C until use. Two µg/mL of D614G spike protein was used to coat 96-well, high-
652 binding plates (Corning) and incubated overnight at 4°C. The plates were incubated in a blocking
653 buffer consisting of 1x PBS, 5% skimmed milk powder, 0.05% Tween 20. Plasma samples were
654 diluted to 1:100 starting dilution in a blocking buffer and added to the plates. IgG secondary
655 antibody (Merck) was diluted to 1:3000 in blocking buffer and added to the plates followed by
656 TMB substrate (Thermofisher Scientific). Upon stopping the reaction with 1 M H2SO4, optical
657 density (OD) was measured at 450 nm. The monoclonal antibodies (mAbs) CR3022 and
658 Palivizumab were used as the positive and negative controls respectively.

659 ## Statistical Analysis

660 **Mediation analyses and household transmission model fitted to observed infections in the**
661 **cohort.**

662 Here we blend concepts from causal inference and infectious disease transmission models. The no
663 interference assumption in causal inference stipulates that the outcome of an individual does not
664 depend on the outcome of others, which is often violated in infectious disease dynamics [36,52,53].
665 This is because the spread of infectious diseases requires pathogens to be transmitted from one
666 host to another. In other words, the infection outcome of one individual inherently depends on the
667 infection outcome of others, and this is particularly pronounced in a household setting [36]. The
668 "dependent happening" nature of infectious disease dynamics violates the no interference
669 assumption. As a result, the traditional regression approach for causal inference analysis cannot be
670 applied to infectious disease outcomes among individuals who can in theory transmit the disease
671 from one to another. To overcome this, Halloran and Struchiner. [36] introduced the probability of

infection conditional on exposure to already infected individuals (transmission probability), as the causal parameter. Using this proposed framework, we can investigate how the presence/absence of pre-existing immunity along with the immunologic marker of interest could modulate probability of infection, after adjusting for levels of exposure to the infectious source(s). The corresponding causal inference framework requires modelling the transmission process explicitly. Under this framework, we conduct mediation analyses to investigate how nAb titers against variants at the start of a SARS-CoV-2 wave correlate with SARS-CoV-2 transmission risk, using the Delta and Omicron BA.1/2 waves as examples [34,35]. We focus on the Delta and Omicron subgroup participants who have had a single or no prior infection, and fit a chain-binoal model to their infection outcomes during the corresponding Delta/Omicron wave [54]. Specifically, we introduce the causal parameters:

- $p_{ij}^{k}$ : the per-contact SARS-CoV-2 household transmission probability from infected individual $i$ to individual $j$ in household $k$.
- $q_{j}^{k}$: the overall probability of acquiring SARS-CoV-2 infection from outside the household by individual $j$ of household $k$ (probability of infection from the community).

We use $e_j$ to indicate individual $j$'s prior SARS-CoV-2 infection history, with $e_j = 0$ representing no prior infection reported before the start of Delta/Omicron BA.1/2 and $e_j = 1$ representing one prior infection by the start of Delta/Omicron BA.1/2 wave. A prior SARS-CoV-2 infection ($e_j = 1$) would induce immunologic responses, measured by a set of immune markers (i.e., candidate mediators) $\{m_j | e_j = 1\}$ (e.g., nAb titers level). Then the household transmission probability $p_{ij}^{k} = p_{ij}^{k}(e_j, \{m_j | e_j = 1\}, \{c_i, c_j, c_k\})$ can be expressed as a function of prior infection status $e_j$, immunologic mediators of SARS-CoV-2 transmission probability $\{m_j | e_j = 1\}$ and additional adjustment terms $\{c_i, c_j, c_k\}$, representing a set of potential confounding factors of individual $i$, individual $j$, and household $k$ (eg, age of the donor and/or recipient, comorbidities, household size, etc). Similarly, the community infection probability $q_j^k = q_j^k(e_j, \{m_j | e_j = 1\}, \{c_j\})$ can be expressed as a function of individual $j$'s prior exposure history $e_j$, immunological markers $\{m_j | e_j = 1\}$, and additional adjustment terms $\{c_j\}$, representing a set of potential confounding factors of individual $j$ (e.g., age or comorbidities).

The causal diagram of the mediation analysis framework is shown in Fig. 3. We fit a household transmission model to the imputed household transmission chains based on an Expectation-maximization (EM) algorithm (detailed in Section 4). Specifically, for the Delta/Omicron BA.1/2 wave, if we look into a specific household $k$ of size $N$, there are a total of $n$ individuals infected belonging to $L$ distinct chains of transmission due to $L$ independent introductions of SARS-CoV-2 into the household. The uninfected individuals are $N - n$. We denote $P_j^k$ the likelihood of any individual $j$ of household $k$ having the observed infection status over the Delta/Omicron BA.1/2 wave (i.e., either infected or not) in a particular realization of the model. There are a few scenarios to write down $P_j^k$:

- Within a given transmission chain $l \in L$, the initial generation $g_j^l = 0$ always has an individual $j$ acquiring infection from the general community (outside the household $k$). Thus, the probability of individual $j$ being infected is $P_j^k = q_j^k$ if $j$ is the first individual to be infected in the chain.
- For infected individual $j$ in the first generation of transmission chain $l$, i.e., $g_j^l = 1$, this individual would have to escape infection risk from the general community but get infected by the infected household member of $g_i^l = 0$. Thus, the probability of individual $j$ being infected can be written as $P_j^k = \left(1 - q_j^k\right) p_{ij}^k$.
- For infected individual $j$ in transmission chain $l$ with generation greater than 1, i.e., $g_l > 1$, this individual has escaped infection risk from the general community as well as infected individuals $i$ two generations away ($g_i^l \leq g_j^l - 2$) but got infected by an infector $i'$ of $j$'s previous generation on the same transmission chain $l$. Thus, the probability of individual $j$ being infected can be written as $P_j^k = \left(1 - q_j^k\right) \times \prod_{i \in \left\{g_i^l \leq g_j^l - 2\right\}} \left(1 - p_{ij}^k\right) \times p_{i'j}^k$.
- For uninfected individual $j$ within household $k$, this individual has escaped infection risk from the general community as well as all the $n$ infected individuals within the same household. Thus, the probability of individual $j$ remaining uninfected can be written as $P_j^k = \left(1 - q_j^k\right) \times \prod_{i \in \{n\}} \left(1 - p_{ij}^k\right)$.

Then, within household $k$ of size $N$, we can express the likelihood of transmission chain $l$ as $\prod_{j \in l} P_j^k$; the likelihood of observing all infections within $k$ can be expressed as $\prod_{l \in L} \prod_{j \in l} P_j^k$; the

likelihood of observing $N-n$ uninfected individuals can be expressed as $\prod_{j\in N-n} P_j^k$. Putting these together, the likelihood of observing one realization of the imputed (details of the EM imputation method described in the next section) households' transmission trees for Delta/Omicron wave can be expressed as:

$$L^{Delta/Omicron} = \prod_k L_k^{Delta/Omicron} \tag{1}$$

Where the likelihood of a given household transmission chains configuration $L_k^{Delta/Omicron}$ can be expressed as:

$$L_k^{Delta/Omicron} = \prod_{l\in L}\prod_{j\in l} P_j^k\left(p_{ij}^k, q_j^k\right) \times \prod_{j\in N-n} P_j^k\left(p_{ij}^k, q_j^k\right) \tag{2}$$

In the remainder of the section, we will consider a few versions of the transmission model with slightly different implementations for $p_{ij}^k$ and $q_j^k$.

**Model 1: waning model for prior exposure with serologically ascertained Delta and Omicron wave infections.**

This is the transmission model presented in the main analysis of the manuscript (results of the model shown in Table 2. In this model, we consider that protection from prior infection unexplained by nAb titers wanes over time but is not dependent on the variant responsible for prior infection (i.e. prior D614G or Beta infections for the Delta wave analysis, and prior D614G, Beta, or Delta infections for the Omicron wave analysis). Additionally, in this model, both the Delta and Omicron wave infections were ascertained by serology based on approach describe in a prior session in Methods.

More specifically, for the Delta wave, $p_{ij}^k$ and $q_j^k$ can be expressed as:

$$p_{ij}^k = \text{expit}\left(\begin{array}{c}\epsilon\left(\frac{1}{2}\right)^{\frac{\Delta t}{\tau}} e_j + \left(\delta_{nAb}^{D614G} m_j^{D614G} + o_{\Delta nAb}^{waning} m_j^{waning}\right)^{e_j} + \lambda e_i + \\ \sum_{c_i\in\{c_i\}} \gamma_{c_i} c_i + \sum_{c_j\in\{c_j\}} \gamma_{c_j} c_j + \sum_{c_k\in\{c_k\}} \gamma_{c_k} c_k + \alpha_s\end{array}\right) \tag{3}$$

$$q_j^k = \text{expit}\left(\begin{array}{c}\epsilon\left(\frac{1}{2}\right)^{\frac{\Delta t}{\tau}} e_j + \left(\delta_{nAb}^{D614G} m_j^{D614G} + o_{\Delta nAb}^{waning} m_{\mathrm{j}}^{waning}\right)^{e_j} + \\ \sum_{c_j \in \{c_j\}} \gamma_{c_j} c_j + \sum_{c_k \in \{c_k\}} \gamma_{c_k} c_k + \beta_s\end{array}\right) \quad (4)$$

As described before, $e_j$ indicates individual $j$'s prior SARS-CoV-2 infection history, with $e_j = 0$ representing uninfected individuals at the start of the Delta wave, $e_j = 1$ representing one prior infection, and $\epsilon$ representing the effect size of the immune protection by prior infection not mediated through anti-D614G nAbs (direct effect, Table 2). $\Delta t$ is the elapsed time between prior infection and blood draw 5 (the blood draw taken prior to the Delta wave which we use in this model) and $\tau$ is the waning half-life of $\epsilon$ (direct effect, Table 2). $m_j^{D614G}$ represents the anti-D614G nAb titer at blood draw 5 and $\delta_{nAb}^{D614G}$ represents the effect size of $m_j^{D614G}$ in mediating infection probability $p_{ij}^k$ against the Delta wave infection (mediator effect, Table 2) at blood draw 5. While $m_j^{waning}$ represents the quantity of anti-D614G nAbs waned from peak level (measured as the highest anti-D614G nAb titer level among the first 5 blood draws) to that at BD5 and $o_{\Delta nAb}^{waning}$ represents the effect size of $m_j^{waning}$ in mediating transmission probability $p_{ji}^k$ against the Delta wave infection (mediator effect, Table 2) at blood draw 5. Note that the term $\delta_{nAb}^{D614G} m_j^{D614G} + o_{\Delta nAb}^{waning} m_j^{waning}$ only exists when $e_j = 1$.

We further evaluate whether breakthrough infections have reduced infectiousness compared to primary infections and may in turn affect $p_{ij}^k$. We use $e_i$ to indicate individual $i$'s (the donor) prior SARS-CoV-2 infection history ($e_i = 0$ means no infection, and $e_i = 1$ represents one prior infection at the start of Delta wave). Further, $\lambda$ represents the effect size of prior infection (in $i$) in reducing the infectiousness of reinfections.

We also consider confounding factors for donor $i$ and recipient $j$, where $c_i$ and $\gamma_{c_i}$ represent infector $i$'s confounding factor ($i$'s age, sex) and effect size, respectively; $c_j$ and $\gamma_{c_j}$ represent $j$'s confounding factor ($j$'s age/sex-specific susceptibility (biology), age/sex- and site-specific susceptibility (behavioral), HIV infection status) and effect size, respectively; $c_k$ and $\gamma_{c_k}$ represent household $k$'s confounding factor (household size) and effect size, respectively. Lastly, $\alpha_s$ and $\beta_s$ are logits of the baseline risks for household and community exposures. All parameters' effect sizes are measured in the log of odds ratios.

Similarly, for the Omicron BA.1/2 wave, $p_{ij}^{k}$ and $q_{j}^{k}$ can be expressed as:

$$p_{ij}^{k} = \text{expit}\left(\begin{array}{c}\epsilon\left(\frac{1}{2}\right)^{\frac{\Delta t}{\tau}} e_j + \left(o_{nAb}^{BA1} m_j^{BA1} + o_{\Delta nAb}^{escape} m_{\mathrm{j}}^{escape}\right)^{e_j} + \lambda e_i + \\ \sum_{c_i \in \{c_i\}} \gamma_{c_i} c_i + \sum_{c_j \in \{c_j\}} \gamma_{c_j} c_j + \sum_{c_k \in \{c_k\}} \gamma_{c_k} c_k + \alpha_s\end{array}\right) \quad (5)$$

$$q_{j}^{k} = \text{expit}\left(\begin{array}{c}\epsilon\left(\frac{1}{2}\right)^{\frac{\Delta t}{\tau}} e_j + \left(o_{nAb}^{BA1} m_j^{BA1} + o_{\Delta nAb}^{escape} m_{\mathrm{j}}^{escape}\right)^{e_j} + \\ \sum_{c_j \in \{c_j\}} \gamma_{c_j} c_j + \sum_{c_k \in \{c_k\}} \gamma_{c_k} c_k + \beta_s\end{array}\right) \quad (6)$$

As described before, $e_j$ indicates individual $j$'s prior SARS-CoV-2 infection history, with $e_j = 0$ representing individual $j$ remained naïve to SARS-CoV-2 at the start of Omicron BA.1/2 wave while $e_j = 1$ representing individual $j$ had one prior infection at the start of Omicron BA.1/2 wave and $\epsilon$ represents the effect size of the immune protection by prior infection not mediated through anti-D614G nAbs (direct effect, Table 2). $\Delta t$ is the elapsed time between prior infection and blood draw 8 (the blood draw taken prior to the Omicron BA.1/2 wave) and $\tau$ is the waning half-life of $\epsilon$ (direct effect, Table 2). Here we consider that parameter $\tau$ is shared between the Delta and Omicron wave and will be jointly estimated (described in the next session in Methods). $m_j^{BA1}$ represents the anti-BA1 nAb titer at blood draw 8 and $o_{nAb}^{BA1}$ represents the effect size of $m_j^{BA1}$ in mediating transmission probability $p_{ji}^{k}$ against the Omicron BA.1/2 wave infection (mediator effect, Table 2) at blood draw 8. While $m_j^{escape}$ represents the difference in titer from anti-D614G nAb to anti-BA1 nAb at blood draw 8 and $o_{\Delta nAb}^{escape}$ represents the effect size of $m_j^{escape}$ in mediating transmission probability $p_{ji}^{k}$ against the Omicron BA.1/2 wave infection (mediator effect, Table 2) at blood draw 8. Note that the term $o_{nAb}^{BA1} m_j^{BA1} + o_{\Delta nAb}^{escape} m_j^{escape}$ only exists when $e_j = 1$. All other parameters have the same definition of the Delta wave.

$\alpha_s$, $\beta_s$, $\epsilon$, $\tau$, $o_{\Delta nAb}^{escape}$, $o_{nAb}^{BA1}$, $\{\gamma_{c_i}\}$, $\{\gamma_{c_j}\}$, $\{\gamma_{c_k}\}$ are estimated through maximizing the likelihood function $L$ for each of the 100 bootstrapped realizations and bootstrap mean and confidence intervals are calculated for each of the parameters.

## Sensitivity analysis

**Model 2: Sensitivity analysis considering variant-specific prior exposure for the direct effects.**

A potential confounding factor in understanding the waning of protection through direct effects is the diversity of prior SARS-CoV-2 exposures, with the dominance of D614G variant in the first wave, Beta variant in the second wave, and Delta variant in the third wave (Fig. 1). The effectiveness of protection may vary depending on the specific variant of prior exposure that induced the immune response at play. We conducted a sensitivity analysis (Model 2) employing a variant-specific model for the direct effects, which accounted for distinct types of SARS-CoV-2 variants conferring prior immunity, instead of considering generic a waning model. Specifically, in Model 2, we considered a more complex version of Model 1, where protection from prior infection depends on the type of infecting variant (i.e. prior D614G or Beta infections for the Delta wave analysis, and prior D614G, Beta, or Delta infections for the Omicron wave analysis). We consider waning in neutralizing titers as in Model 1, but we eliminate waning in the effect of prior infection that is not captured by neutralizing titers. More specifically, for the Delta wave, $p_{ij}^{k}$ and $q_{j}^{k}$ can be expressed as:

$$p_{ij}^{k} = \text{expit}\left(\begin{array}{c}\epsilon^{D614G} e_j^{D614G} + \epsilon^{Beta} e_j^{Beta} + \left(\delta_{nAb}^{D614G} m_j^{D614G} + o_{\Delta nAb}^{waning} m_{\mathrm{j}}^{waning}\right)^{e_j} + \lambda e_i + \\ \sum_{c_i \in \{c_i\}} \gamma_{c_i} c_i + \sum_{c_j \in \{c_j\}} \gamma_{c_j} c_j + \sum_{c_k \in \{c_k\}} \gamma_{c_k} c_k + \alpha_s\end{array}\right) \quad (7)$$

$$q_{j}^{k} = \text{expit}\left(\begin{array}{c}\epsilon^{D614G} e_j^{D614G} + \epsilon^{Beta} e_j^{Beta} + \left(\delta_{nAb}^{D614G} m_j^{D614G} + o_{\Delta nAb}^{waning} m_{\mathrm{j}}^{waning}\right)^{e_j} + \\ \sum_{c_j \in \{c_j\}} \gamma_{c_j} c_j + \sum_{c_k \in \{c_k\}} \gamma_{c_k} c_k + \beta_s\end{array}\right) \quad (8)$$

Here, $e_j^{D614G(Beta)} = 1$ indicates individual $j$, prior to the Delta wave, was infected with D614G (Beta) variant. If $e_j^{D614G} = e_j^{Beta} = 0$, individual $j$ was naïve at the beginning of the Delta wave. $\epsilon^{D614G}$ and $\epsilon^{Beta}$ represent the effect size of immune protection by prior D614G and Beta infection not mediated through anti-D614G nAbs, respectively.

For the Omicron wave, $p_{ij}^{k}$ and $q_{j}^{k}$ can be expressed as:

$$p_{ij}^{k} = \text{expit}\left(\begin{array}{c}\epsilon^{D614G} e_j^{D614G} + \epsilon^{Beta} e_j^{Beta} + \epsilon^{Delta} e_j^{Delta} + \left(o_{nAb}^{BA1} m_j^{BA1} + o_{\Delta nAb}^{escape} m_{\mathrm{j}}^{escape}\right)^{e_j} + \lambda e_i + \\ \sum_{c_i \in \{c_i\}} \gamma_{c_i} c_i + \sum_{c_j \in \{c_j\}} \gamma_{c_j} c_j + \sum_{c_k \in \{c_k\}} \gamma_{c_k} c_k + \alpha_s \end{array}\right) \quad (9)$$

$$q_{j}^{k} = \text{expit}\left(\begin{array}{c}\epsilon^{D614G} e_j^{D614G} + \epsilon^{Beta} e_j^{Beta} + \epsilon^{Delta} e_j^{Delta} + \left(o_{nAb}^{BA1} m_j^{BA1} + o_{\Delta nAb}^{escape} m_{\mathrm{j}}^{escape}\right)^{e_j} + \\ \sum_{c_j \in \{c_j\}} \gamma_{c_j} c_j + \sum_{c_k \in \{c_k\}} \gamma_{c_k} c_k + \beta_s \end{array}\right) \quad (10)$$

Here, $e_j^{D614G(Beta,Delta)} = 1$ indicates individual $j$, prior to the Omicron wave, was infected with D614G (Beta, Delta) variant. If $e_j^{D614G} = e_j^{Beta} = e_j^{Delta} = 0$, individual $j$ was naïve at the beginning of the Omicron wave. $\epsilon^{D614G}$, $\epsilon^{Beta}$ and $\epsilon^{Delta}$ represent the effect size of the immune protection by prior D614G, Beta and Delta infection not mediated through anti-D614G nAbs, respectively.

Additionally, similarly to Model 1, both the Delta and Omicron wave infections were ascertained by serology for Model 2. All other settings of Model 2 were kept the same as Model 1. The results of the Model 2 are presented in Extended Data Table 2.

Our analysis revealed that for both the Delta and Omicron waves, more recent variants conferred stronger protection than earlier variants, albeit with overlapping confidence intervals (Extended Data Table 2). This temporal trend aligns with the expectations of the waning model. Both waning and variant-specific immunity may modulate the direct effects of prior immunity; however, our study lacked sufficient statistical power to jointly estimate the relative contributions of these two factors. Full estimates of this sensitivity analyses are presented in Extended Data Table 2.

**Model 3: Sensitivity analysis with Delta wave infections ascertained by PCR and/or serology.**

For Model 1, both the Delta and Omicron wave infection outcomes were inferred using the kinetics of anti-nucleocapsid antibodies from longitudinal serologic sampling, as detailed in previously published studies of the PHIRST-C cohort [30,32]. This approach for inferring infections based on serology was calibrated against virological evidence of infection during the Delta wave, established through twice-weekly rRT-PCR tests regardless of symptom presentation. However, it should be noted that this calibration did not achieve perfect concordance; the serology approach demonstrated 93% sensitivity and 89% specificity when compared to infections identified by rRT-

PCR tests [30]. To address the uncertainties arising from the imperfect concordance between the two approaches for ascertaining infections, we conducted a sensitivity analysis (Model 3) for the Delta wave, where we considered infections based on rRT-PCR positivity and/or anti-nucleocapsid antibody serology. We identified an additional 17 infections during the Delta wave through this more sensitive infection ascertainment approach, bringing the total number of Delta wave infections to 290. All other settings of Model 3 were kept the same as Model 1. The results of the Model 3 are presented in Extended Data Table 3.

Notably, estimates of the direct and indirect effects of the mediation analysis were comparable between this sensitivity analysis and the main analysis (compare Extended Data Table 3 to Table 1). These findings provide support for the utilization of anti-nucleocapsid serology to ascertain Omicron BA.1/2 wave infections in the studied cohorts, in a period where twice-weekly rRT-PCR testing was not available and confirms the robustness of our CoP analyses.

**Model 4: D614G spike binding antibodies as mediators of protection.**

We conducted sensitivity analysis (Model 4) to explore the role of D614G spike binding antibodies (referred to as bAb hereafter), as potential correlates of protection for both Delta and Omicron infections. Employing an in-house enzyme-linked immunosorbent assay (ELISA), we quantified the level of D614G spike bAb based by measuring absorbance at 450nm at an optical density (OD) at peak levels and BD5 (DB8) for the Delta (Omicron) wave analysis (Extended Data Fig. 3). The reduction in binding antibody levels from peak ($\Delta bAb^{W}$) was determined as the difference between OD values at peak and BD5 (BD8) for the Delta (Omicron) wave (Extended Data Fig. 3).

Model 4 builds on Model 2 but replaces nAb titers with D614G spiking binding ELISA readouts as mediators of protection, in order to compare the protection afforded by neutralizing vs binding antibodies. More specifically, for the Delta wave, $p_{ij}^{k}$ and $q_{j}^{k}$ can be expressed as:

$$p_{ij}^{k} = \text{expit}\left(\begin{array}{c}\epsilon^{D614G} e_j^{D614G} + \epsilon^{Beta} e_j^{Beta} + \left(\delta_{bAb}^{D614G} m_j^{D614G} + o_{\Delta bAb}^{waning} m_{\mathrm{j}}^{waning}\right)^{e_j} + \lambda e_i + \\ \sum_{c_i \in \{c_i\}} \gamma_{c_i} c_i + \sum_{c_j \in \{c_j\}} \gamma_{c_j} c_j + \sum_{c_k \in \{c_k\}} \gamma_{c_k} c_k + \alpha_s\end{array}\right) \quad (11)$$

$$q_{j}^{k} = \text{expit}\left(\begin{array}{c}\epsilon^{D614G} e_j^{D614G} + \epsilon^{Beta} e_j^{Beta} + \left(\delta_{bAb}^{D614G} m_j^{D614G} + o_{\Delta bAb}^{waning} m_{\mathrm{j}}^{waning}\right)^{e_j} + \\ \sum_{c_j \in \{c_j\}} \gamma_{c_j} c_j + \sum_{c_k \in \{c_k\}} \gamma_{c_k} c_k + \beta_s\end{array}\right) \quad (12)$$

Here, $m_j^{D614G}$ represents the D614G spike binding antibodies ELISA readout at blood draw 5 and $\delta_{bAb}^{D614G}$ represents the effect size of $m_j^{D614G}$ in mediating transmission probability $p_{ij}^k$ against the Delta wave infection at blood draw 5. Further, $m_j^{waning}$ represents the drop from peak D614G spike binding antibodies readout prior to blood draw 5 (measured as the highest D614G spike binding Ab titer level among the first 5 blood draws) to that at blood draw 5 and $o_{\Delta bAb}^{waning}$ represents the effect size of $m_j^{waning}$ in mediating transmission probability $p_{ji}^k$ against the Delta wave infection at blood draw 5.

For the Omicron wave, $p_{ij}^k$ and $q_j^k$ can be expressed as:

$$p_{ij}^k = \text{expit}\left(\begin{array}{c}\epsilon^{D614G} e_j^{D614G} + \epsilon^{Beta} e_j^{Beta} + \epsilon^{Delta} e_j^{Delta} + \\ \left(\delta_{bAb}^{D614G} m_j^{D614G} + o_{\Delta bAb}^{waning} m_{\mathrm{j}}^{waning}\right)^{e_j} + \lambda e_i + \\ \sum_{c_i \in \{c_i\}} \gamma_{c_i} c_i + \sum_{c_j \in \{c_j\}} \gamma_{c_j} c_j + \sum_{c_k \in \{c_k\}} \gamma_{c_k} c_k + \alpha_s\end{array}\right) \tag{13}$$

$$q_j^k = \text{expit}\left(\begin{array}{c}\epsilon^{D614G} e_j^{D614G} + \epsilon^{Beta} e_j^{Beta} + \epsilon^{Delta} e_j^{Delta} + \\ \left(\delta_{bAb}^{D614G} m_j^{D614G} + o_{\Delta \mathrm{bAb}}^{waning} m_{\mathrm{j}}^{waning}\right)^{e_j} + \\ \sum_{c_j \in \{c_j\}} \gamma_{c_j} c_j + \sum_{c_k \in \{c_k\}} \gamma_{c_k} c_k + \beta_s\end{array}\right) \tag{14}$$

Here, $m_j^{D614G}$ represents the D614G spike binding antibodies ELISA readout at blood draw 8 and $\delta_{bAb}^{D614G}$ represents the effect size of $m_j^{D614G}$ in mediating transmission probability $p_{ij}^k$ against the Omicron wave infection at blood draw 8. While $m_j^{waning}$ represents the drop from peak D614G spike binding antibodies readout prior to blood draw 8 (measured as the highest D614G spike binding Ab titer level among the first 8 blood draws) to that at blood draw 8 and $o_{\Delta bAb}^{waning}$ represents the effect size of $m_j^{waning}$ in mediating transmission probability $p_{ji}^k$ against the Omicron wave infection at blood draw 8. All other settings of Model 4 were kept the same as Model 2. The results of the Model 4 are presented in Extended Data Table 4.

We found that binding antibody levels at BD5 (BD8) correlate with protection against Delta (Omicron) wave infections: the risk of infection decreased by 74% (95% CI 41% – 88%) and 40% (95% CI 33% – 54%) per unit increase in OD value for the Delta and Omicron wave analyses,

respectively. Conversely, the decline in bAbs from peak levels to BD5/BD8 ( $\Delta bAb^{W}$ ) demonstrated no contribution to the overall protection, with risk reduction per 10-fold increase: -2% (95%CI: -91% – 55%) for Delta wave infections and -2% (95%CI: -87% – 55%) for Omicron wave infections. These findings underscore the correspondence between waning of binding antibodies and a waning of protection. Furthermore, our estimations indicate that the proportion of protection conferred through D614G spike bAbs at BD5 is 35% (95%CI: 32% – 38%) against Delta wave infections, a figure comparable estimation based on anti-D614G nAbs (37%, 95%CI: 34% – 40%, Extended Data Table 4). Notably, D614G spike bAbs at BD8 accounted for 27% (95% CI: 25% – 29%) of protection against Omicron wave infection, representing a larger proportion compared to anti-BA.1 nAbs (11%, 95%CI: 9% – 12%, Extended Data Table 4).

## Transmission chains imputation and parameters estimation based on an Expectation-maximization (EM) algorithm.

Here we describe the process to fit the models described in Section 3 to the household infection data. The serologic data available for the Delta and Omicron only provides information on the total number of infections within the household between two blood draws collected before and after the SARS-CoV-2 wave. The data does not provide the details of the transmission chains within the household, the order of infections among infected individuals, nor the infection dates. To account for the uncertainties of the transmission tree structure within households given only the total number of infections, we enumerate and reconstruct all possible transmission chains among the infected individuals, where each infected individual may have been infected by members of their own household or the general community. Supplementary Fig. 1 illustrates all 16 possible configurations of transmission chains for a household with 3 infected individuals. We limited our analysis to households with no more than 6 infected individuals, as the possible configurations of transmission chains among 6 infected individuals already reaches 16,807. Enumeration of all possible transmission chain configurations would be computationally intractable for households with more than 6 infected individuals. Additionally, the probability of each possible transmission chain depends on the parameter estimates of the transmission model described in the previous session in Methods. To address the statistical uncertainties due to unresolved transmission chains (which would affect the statistical confidence of mediation analysis detailed in the prior section),

we jointly fit the household transmission model and impute the topological structure of the transmission trees. We use an EM algorithm, as described below [55].

To resolve who infected whom within the household in a probabilistic manner, we considered an EM algorithm that iteratively estimates the transmission model parameters $\alpha_s$, $\beta_s$, $\epsilon$, $\tau$, $\delta_{nAb}^{D614G/BA1}$, $o_{\Delta nAb}^{waning/escape}$, $\{\gamma_{c_i}\}$, $\{\gamma_{c_j}\}$, $\{\gamma_{c_k}\}$ through maximizing the likelihood function $L$ as described in Equation (1) in the previous section then updates the imputed probability of each transmission tree configuration within each household based on the fitted transmission model. The process is as follows:

(1) Initial imputation of the household transmission trees with equal sampling probability for all configurations: For each household, we randomly sample one transmission tree with equal probability among all transmission tree configurations that are compatible with the number of infections. We iterate through all households so that each household has a simulated transmission tree. We then repeat the imputation 1000 times to obtain 1000 realizations of each household's transmission tree.

(2) Maximization step: We consider the waning parameter $\tau$ a hyper-parameter (nonlinear term in equations (3-6), cannot be estimated by logistic regression). For a fixed value of $\tau$, for each of the 1000 realizations of the simulated household transmission chains, we estimate transmission model parameters $\alpha_s$, $\beta_s$, $\epsilon$, $\delta_{nAb}^{D614G/BA1}$, $o_{\Delta nAb}^{waning/escape}$, $\{\gamma_{c_i}\}$, $\{\gamma_{c_j}\}$, $\{\gamma_{c_k}\}$ through maximizing the likelihood function $L$ described in Equation (1). The maximization of the likelihood function is achieved through fitting a logistic regression of the infection/exposure outcomes for all participants using R package ***"brglm"*** (version 0.7.2). We then pool the estimates from the 1000 realizations using the ***"pool"*** function in the R package ***"mice"*** (version 3.16.0). The full likelihood of the combined Delta and Omicron waves fitting in this EM step $m$ can be expressed as $L_m(\tau) = L_m^{Delta}(\tau) \times L_m^{Omicron}(\tau)$

(3) Expectation step: for a fixed value of hyper-parameter $\tau$, based on the pooled estimates of the transmission model parameters $\alpha_s$, $\beta_s$, $\epsilon$, $\delta_{nAb}^{D614G/BA1}$, $o_{\Delta nAb}^{waning/escape}$, $\{\gamma_{c_i}\}$, $\{\gamma_{c_j}\}$, $\{\gamma_{c_k}\}$, we calculate the likelihood all configurations of transmission chains within each household based on Equation (2). We use these configuration-specific likelihoods to resample

transmission chains: For each household, we randomly sample one transmission tree among all transmission tree configurations with probability proportional to transmission tree likelihood prescribed in Equation (2), given the parameters estimated by the most recent maximization step. We iterate through all households so that each household is assigned one simulated transmission tree. We repeat the process 1000 times to obtain 1000 realizations of the household transmission trees.

(4) For each of the fixed value of hyper-parameter $\tau$ over a plausible range (30 - 500 days), we iterate over the EM steps (2) and (3) until $L_m(\tau)$ converge to the maximum value of the EM algorithm. We scan through the values of $\tau$ from 30 to 500 days at 10 days step. The EM algorithm convergence curve is shown in Supplementary Fig. 2 for each of the $\tau$ values. The EM algorithm converges at step 50, irrespective of the value of $\tau$. The marginal likelihood of the model at $\tau$, $L(\tau)$ is estimated by taking the average of $L_m(\tau)$ for EM steps 50 through 100. Supplementary Fig. 3 shows the log of the likelihood $L(\tau)$ as a function of $\tau$, based on a spline interpolation. The point estimate of $\tau$ is taken from the maximum of $\log\big(L(\tau)\big)$ while the 95% confidence interval is estimated by finding $\tau$ values with log-likelihood value at the maximum minus 1.92 (Supplementary Fig. 3).

(5) We then take the best estimate of hyper-parameter $\tau$ and repeat the EM algorithm till convergence to estimate transmission model parameters $\alpha_s$, $\beta_s$, $\epsilon$, $\delta_{nAb}^{D614G/BA1}$, $o_{\Delta nAb}^{waning/escape}$,$\{\gamma_{c_i}\}$, $\{\gamma_{c_j}\}$, $\{\gamma_{c_k}\}$ as show in Table 2. Same EM algorithm were applied to Model 2-4 for the sensitivity analysis as well.

The "treatment effect" by prior infection is estimated by simulating from the best-fit model. We first sample 1000 realizations of the imputed household transmission trees, with imputation probability proportional to the best estimates of transmission model using the EM algorithm and hyper-parameter $\tau$. For each of the 1000 realizations, we focus on the subset of individuals who had one prior SARS-CoV-2 infection, denoted as $S_j = \{j|\ e_j = 1\}$). We use the fitted transmission model to predict the probability of infection (i.e. $P_j = p_{ij}^k\ or\ q_j^k$, with ) of these non-naïve subsets under three scenarios:

a. Scenario 1: the probability of infection estimated with predictors as reported in the data, denoted as $P_j^{obs}$.

b. Scenario 2: a counterfactual scenario where the probability of infection is estimated with predictor $e_j = 0$ (i.e. a counterfactual naïve individual) whereas all other covariates (confounders) are the same as observed, removing both direct and mediator effects. We denote the infection probability in this counterfactual scenario as $P_j^{\text{counterfactual}}\left(e_j = 0\right)$.

c. Scenario 3: a counterfactual scenario where the probability of infection is estimated with predictor $e_j = 1$, but setting $m_{nAb}^{BA1} = 0$ (or $m_{nAb}^{D614G} = 0$), effectively removing the mediator effect of nAb on preventing transmission, but keeping the direct effect. We denote the infection probability in this counterfactual scenario as $P_j^{\text{counterfactual}}\left(e_j = 1;\ m_{nAb} = 0\right)$.

We then calculate the total protection conferred by prior infection as the population average of $P_j^{\text{counterfactual}}\left(e_j = 0\right)/P_j^{obs}$, based on bootstrap resampling with replacement (maintaining the same number of observations) of each of the 1000 realizations of the household transmission chains. Point estimates and 95% confidence intervals are based on the median and 95% quantiles of 1000 realizations' estimates.

Similarly, we calculate the proportion of protection mediated by nAbs as the population average of $1 - \frac{P_j^{\text{counterfactual}}\left(e_j=1;\ m_{nAb}=0\right)/P_j^{obs}}{P_j^{\text{counterfactual}}\left(e_j=0\right)/P_j^{obs}}$. We use the same bootstrapping approach as for total protection.

## Data availability

Aggregate data to reproduce the figures are available at Zenodo (DOI: 10.5281/zenodo.11375487). Individual-level data cannot be publicly shared because of ethical restrictions and the potential for identifying included individuals. Accessing individual participant data and a data dictionary defining each field in the dataset would require provision of protocol and ethics approval for the proposed use. To request individual participant data access, please submit a proposal to C.C (cherylc@nicd.ac.za). who will respond within 1 month of request. Upon approval, data can be made available through a data sharing agreement.

## Code availability

Code to reproduce the figures, using python version 3.8.11 and scipy version 1.7.1 is available at Zenodo (DOI: 10.5281/zenodo.11375487).

1009 # Extended Data Figures:

1010

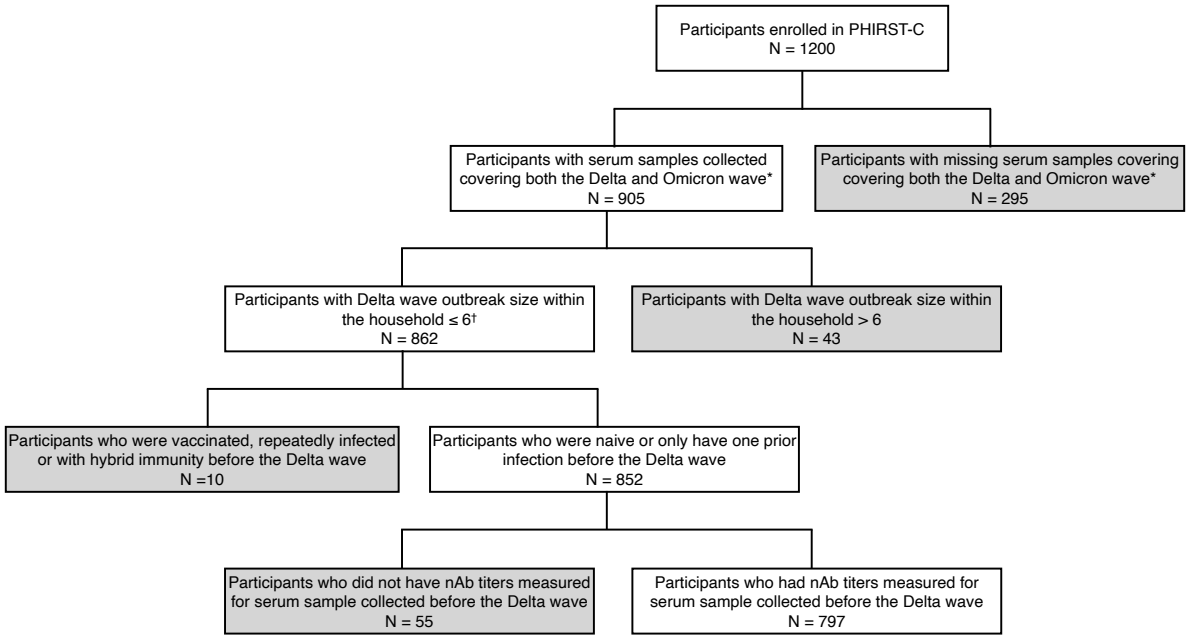


1011

1012 **Extended Data Fig. 1:** Flowchart of participants included in the Delta-wave subgroup analysis. Grey boxes represent
1013 participants excluded from the Delta-wave subgroup analysis.

1014 *Based on a previously published study [30].

1015 †Household with more than 6 infected individuals would be computationally intractable to track all possible
1016 transmission chain configurations.

1017

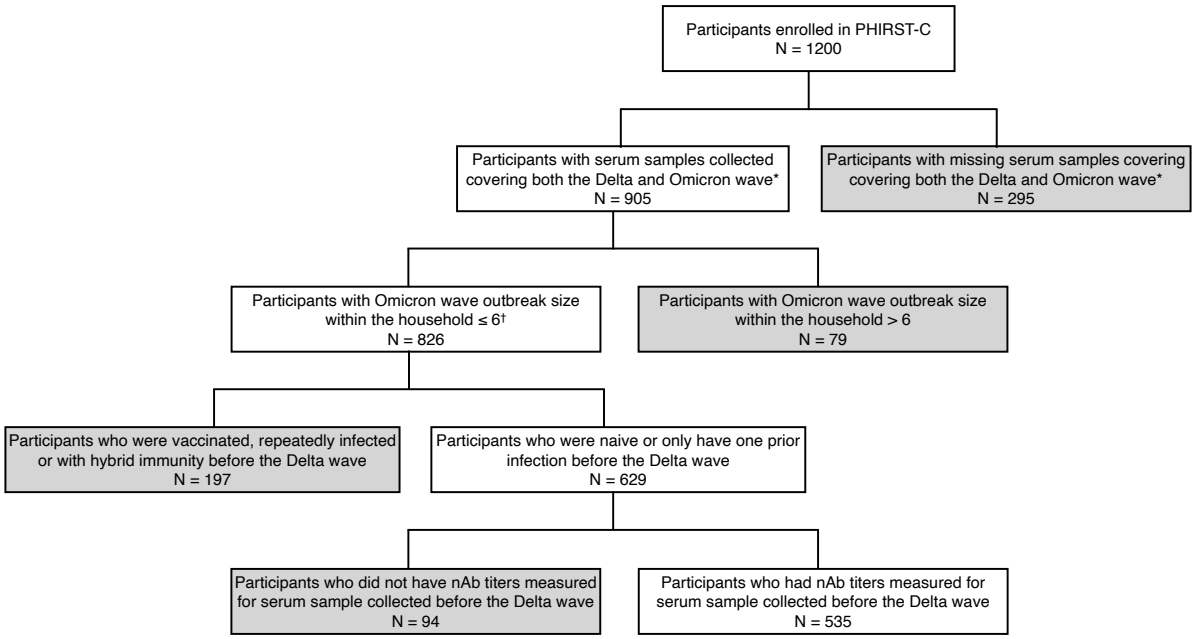


**Extended Data Fig. 2:** Flowchart of participants included in the Omicron-wave subgroup analysis. Grey boxes represent participants excluded from the Omicron-wave subgroup analysis.

*Based on a previously published study [30].

†Household with more than 6 infected individuals would be computationally intractable to track all possible transmission chain configurations.

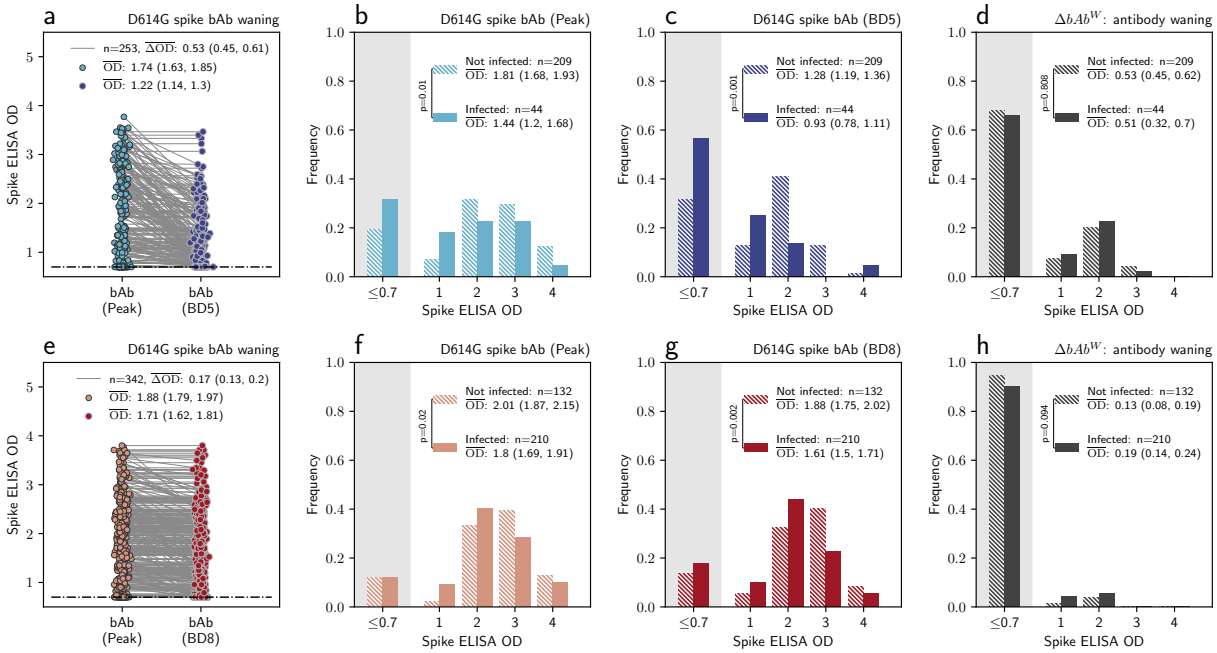


**Extended Data Fig. 3: D614G spike binding antibody (bAb) level for the Delta wave and the Omicron wave analysis. a**, for Delta wave subgroup, the distribution of the peak bAb level to BD5 (light blue dots) and the D614G spike bAb level at BD5 (dark blue dots), among individuals who had one prior SARS-CoV-2 infection before blood draw 5. Each dot represents one individual, with two measurements of the same individual connected through a gray line. OD: absorbance at 450 nm, measured in optical density; $\overline{OD}$: the average of OD; $\overline{\Delta OD}$: the average drop of OD. **b**, for Delta wave subgroup, the distribution of the peak D614G spike bAb up to BD5, stratified by individuals who were infected during the Delta wave (solid bar) vs those who were not infected (dashed bar). Independent samples t-test (two-sided) is used to determine the statistical significance (anti reported on the legend) of difference between the $\overline{OD}$ of the two groups. **c**, same as **b** but for D614G spike bAb level at BD5. **d**, same as **b** but for $\Delta bAb^W$. **e**, for Omicron wave subgroup, the distribution of the peak bAb level to BD8 (light red dots) and the D614G spike bAb level at BD8 (dark red dots), among individuals who had one prior SARS-CoV-2 infection before BD8. Each dot represents one individual, with two measurements of the same individual connected through a gray line. **f**, for the Omicron wave subgroup, the distribution of the D614G spike bAb level at BD8, stratified by individuals who were infected during the Omicron wave (solid bar) vs those who were not infected (dashed bar). Independent samples t-test (two-sided) is used to determine the statistical significance (p-value reported on the legend) of difference between the $\overline{OD}$s of the two groups. **g**, same as **f** but for D614G spike bAb level at BD8. **d**, same as **f** but for $\Delta bAb^W$.

1043 # Extended Data Tables:

1044 **Extended Data Table 1: Positivity rate of different serologic assays by the variant type of prior exposure for the**
1045 **Delta and Omicron wave subgroup.**

| **Delta wave subgroup** | | | |
|---|---|---|---|
| **Seropositivity** | **Prior D614G infection** | **Prior Beta infection** | **Prior Delta exposure** |
| Anti-nucleocapsid assay were positive in at least one of the first 5 blood draws | 109/113 (97%) | 133/140 (95%) | – |
| Anti-nucleocapsid assay were positive at BD5 | 104/113 (92%) | 129/140 (92%) | – |
| Anti-D614G nAb assay were positive for peak nAb response. | 87/113 (77%) | 60/140 (43%) | |
| Anti-D614G nAb were positive for nAb response at BD5 | 81/113 (72%) | 59/140 (42%) | – |
| **Omicron wave subgroup** | | | |
| **Seropositivity** | **Prior D614G exposure** | **Prior Beta exposure** | **Prior Delta exposure** |
| Anti-nucleocapsid assay were positive in at least one of the first 8 blood draws | 60/61 (98%) | 116/120 (97%) | 160/161 (99%) |
| Anti-nucleocapsid assay were positive at BD8 | 58/61 (95%) | 108/120 (90%) | 159/161 (99%) |
| Anti-D614G nAb were positive for nAb response at BD8 | 57/61 (93%) | 71/120 (59%) | 140/161 (87%) |
| Anti-BA.1 nAb were positive for nAb response at BD8 | 29/61 (48%) | 36/120 (30%) | 50/161 (31%) |

1046

**Extended Data Table 2: Mediation analysis for nAbs as CoPs against serologically ascertained Delta and Omicron wave infections, with a variant-specific model for direct effect.** Average and 95% CIs are provided for each of the model parameters. $\Delta nAb^{W}$: the quantity of anti-D614G nAbs waned from peak level to that at BD5. $\Delta nAb^{E}$: the quantity of antibodies that can neutralize D614G but fail to neutralize Omicron BA.1 at BD8 due to Omicron's immune escape.

| **Wave** | | | Delta | Omicron |
|---|---|---|---|---|
| **Protection against reinfection** | **Direct effect** (Protection absent of nAbs) | **Prior D614G exposure** (odds ratio, absent of waning) | 0.76 (0.36, 1.61) | 1.23 (0.63, 2.38) |
| | | **Prior Beta exposure** (odds ratio, absent of waning) | 0.47 (0.30, 0.76) | 0.78 (0.50, 1.21) |
| | | **Prior Delta exposure** (odds ratio, absent of waning) | – | 0.47 (0.29, 0.76) |
| | **Mediators effect** (Protection from nAbs) | **Anti-D614G nAb** (odds ratio, per 10-fold increase) | 0.59 (0.43, 0.83) | – |
| | | $\boldsymbol{\Delta nAb^{W}}$ (odds ratio, per 10-fold increase) | 1.00 (0.72, 1.39) | – |
| | | **Anti-BA.1 nAb** (odds ratio, per 10-fold increase) | – | 0.73 (0.56, 0.95) |
| | | $\boldsymbol{\Delta nAb^{E}}$ (odds ratio, per 10-fold increase) | – | 0.94 (0.76, 1.15) |
| | **Total protection** (relative risk compared to naïve individuals) | | 0.40 (0.38, 0.42) | 0.70 (0.68, 0.72) |
| | **Proportion of protection mediated by nAbs** | | 37% (34%, 40%) | 11% (9%, 12%) |
| **Protection against onward transmission** (Odds ratio compared to naïve individuals) | | | 0.20 (0.05, 0.72) | 1.11 (0.62, 2.00) |

**Extended Data Table 3: Mediation analysis for nAbs as CoPs against Delta (ascertained by both serology and PCR) and Omicron wave infections, with a waning model for direct effect.** Average and 95% CIs are provided for each of the model parameters. $\Delta nAb^{W}$: the quantity of anti-D614G nAbs waned from peak level to that at BD5. $\Delta nAb^{E}$: the quantity of antibodies that can neutralize D614G but fail to neutralize Omicron BA.1 at BD8 due to Omicron's immune escape.

| **Wave** | | | Delta | Omicron |
|---|---|---|---|---|
| **Protection against reinfection** | **Direct effect** (Protection absent of nAbs) | **Effect size** (odds ratio, absent of waning) | 0.34 (0.17, 0.64) | 0.29 (0.17, 0.51) |
| | | **Waning half-life** (days) | 128 (77, 261) | |
| | **Mediators effect** (Protection from nAbs) | **Anti-D614G nAb** (odds ratio, per 10-fold increase) | 0.65 (0.49, 0.86) | – |
| | | $\boldsymbol{\Delta nAb^{W}}$ (odds ratio, per 10-fold increase) | 1.02 (0.78, 1.36) | – |
| | | **Anti-Omicron BA.1 nAb** (odds ratio, per 10-fold increase) | – | 0.73 (0.56, 0.95) |
| | | $\boldsymbol{\Delta nAb^{E}}$ (odds ratio, per 10-fold increase) | – | 1.01 (0.84, 1.21) |
| | **Total protection** (relative risk compared to naïve individuals) | | 0.41 (0.40, 0.43) | 0.62 (0.61, 0.64) |
| | **Proportion of protection mediated by nAbs** | | 33% (30%, 35%) | 11% (9%, 12%) |
| **Protection against onward transmission** (Odds ratio compared to naïve individuals) | | | 0.23 (0.08, 0.71) | 1.19 (0.66, 2.13) |

**Extended Data Table 4: Mediation analysis for D614G spike binding antibody as CoPs against serologically ascertained Delta and Omicron wave infections, with a variant-specific model for direct effect.** Average and 95% CIs are provided for each of the model parameters. $\Delta bAb^{W}$: the quantity of D614G spike binding antibodies waned from peak level to that at BD5 for Delta (at BD8 for Omicron).

| **Protection against reinfection** | | | Delta (serology) | Omicron (serology) |
|---|---|---|---|---|
| | **Direct effect** (Protection absent of nAbs) | **Prior D614G exposure** (odds ratio, absent of waning) | 0.60 (0.24, 1.48) | 1.38 (0.67, 2.84) |
| | | **Prior Beta exposure** (odds ratio, absent of waning) | 0.51 (0.32, 0.83) | 0.91 (0.58, 1.45) |
| | | **Prior Delta exposure** (odds ratio, absent of waning) | – | 0.61 (0.38, 0.97) |
| | **Mediators effect** (Protection from nAbs) | **D614G binding Ab** (odds ratio, per 10-unit increase) | 0.26 (0.12, 0.59) | 0.60 (0.46, 0.77) |
| | | **$\Delta bAb^{W}$** (odds ratio, per 10-unit increase) | 1.02 (0.55, 1.91) | 1.02 (0.55, 1.87) |
| | **Total protection** (relative risk compared to naïve individuals) | | 0.40 (0.38, 0.42) | 0.65 (0.63, 0.67) |
| | **Proportion of protection mediated by spike binding Ab** | | 35% (32%, 38%) | 27% (25%, 29%) |
| **Protection against onward transmission** (Odds ratio compared to naïve individuals) | | | 0.22 (0.06, 0.74) | 1.18 (0.65, 2.13) |

# Supplementary Information

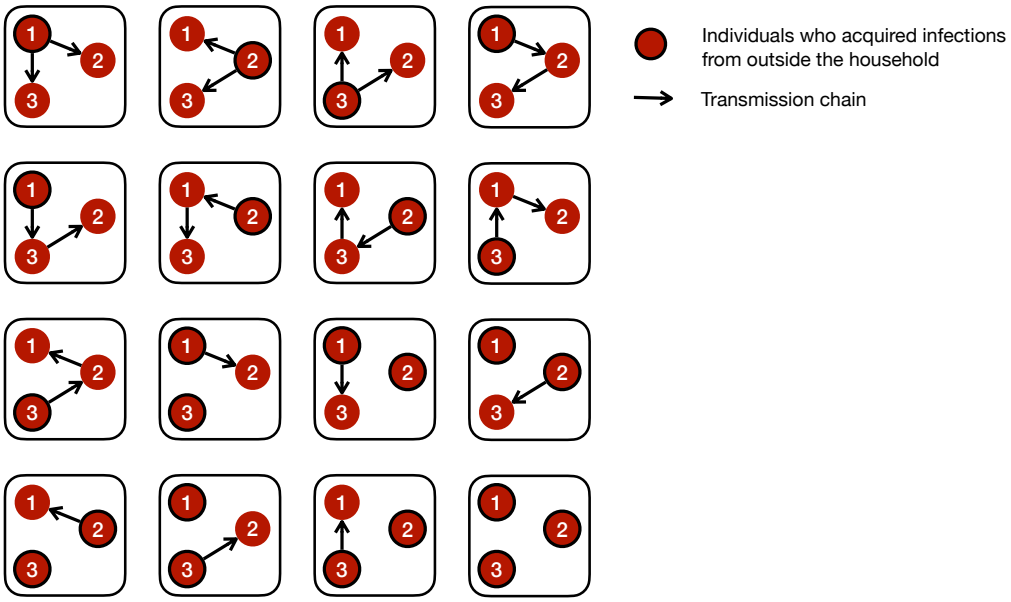


**Supplementary Fig. 1:** Visualization of all 16 possible transmission chains within a household of 3 infected individuals.

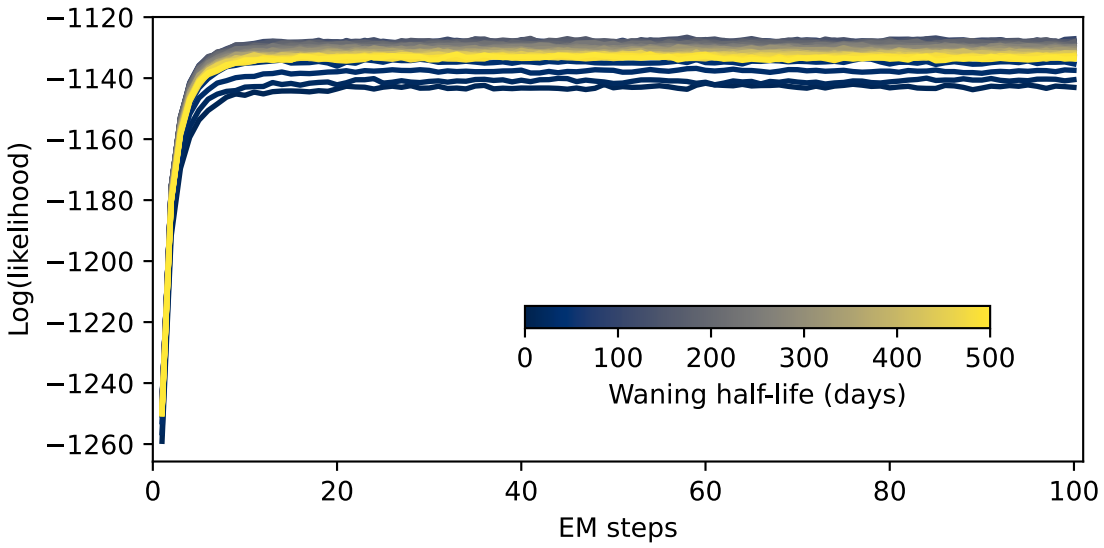


**Supplementary Fig. 2: The log-likelihood of the transmission model fit, as a function of the EM steps.**

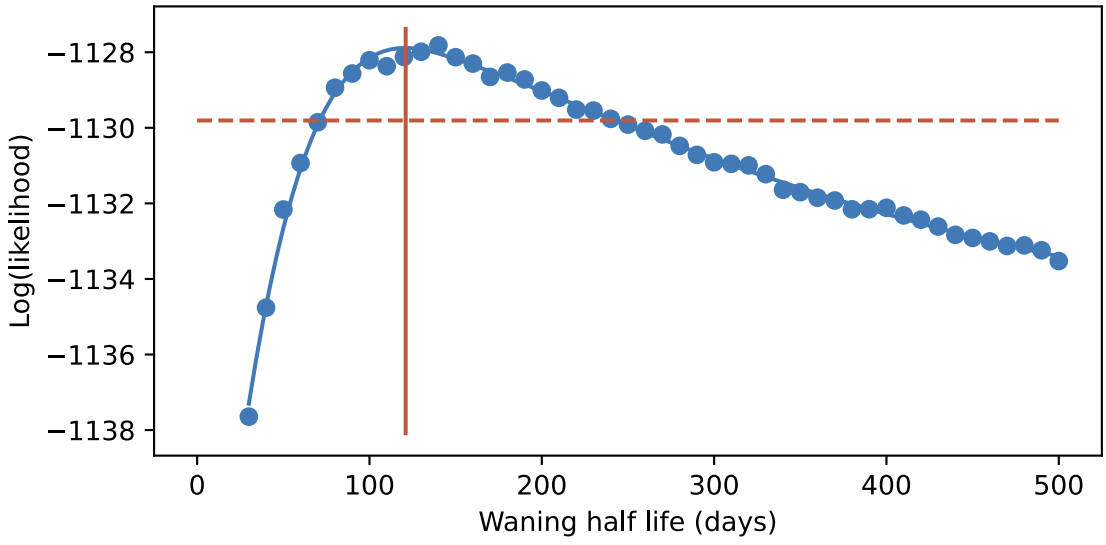


**Supplementary Fig. 3: The profile log-likelihood of the transmission model over hyper-parameter of waning half-life.** Solid vertical line indicates the waning half-life corresponding to maximum of the profile likelihood. Dashed horizontal line represent 1.92 below the maximum profile likelihood.